Development of Root Hairs is aligned with the Tolerance Trait of Cotton against the Infections of *Rotylenchulus Reniformis*, Plant Parasitic Nematode

by

Heather Nicole Gosse

A thesis submitted to the Graduate Faculty of
Auburn University
in partial fulfillment of the
requirements for the Degree of
Master of Science

Auburn, Alabama
December 15, 2018

Approved by

Dr. Sang-Wook Park, Chair, Assistant Professor of Entomology and Plant Pathology
Dr. John Murphy, Professor of Entomology and Plant Pathology
Dr. Aaron Rashotte, Associate Professor of Biological Sciences

ABSTRACT

Plant parasitic nematodes (PPN) are major cotton pathogens, causing the annual yield of up to 10 % annually. Lately, reniform nematode (RN, *Rotylenchulus reniformis*) has become a major threat to the cotton farming industry across the southeastern US region. However, current pest management programs lack a) resistant cultivar, b) efficacious rotation crop, and c) effective and low cost nematicide, and is in urgent need of breakthrough but it is not necessarily forthcoming due to a narrow genetic diversity in the cotton cultivars and germplasm, as well as little knowledge on the pathophysiology of cotton-PPN interactions.

Generally used to tag or probe stained targeted materials, fluorescent chemical compounds are useful in most -if not all- areas of basic and applied sciences. Epi-fluorescence microscopy unveiled that RN produce autofluorescence compounds in intestinal areas. Characterization techniques were implemented to better understand multifluorescent molecule including observational studies to determine autofluorescence resides in intestinal tract and affluent throughout lifecycle. Stabilization tests incubating autofluorescence in various H_2O_2, DTT and pH concentrations using the Cytation 3 Image Reader ^{TM}, showed to be overall stable. Structural identification using high performance liquid chromatography, mass septectomy and nuclear magnetic resonance was found to be Sulfonium, [(17β) -3-ethoxyestra-1,3,5(10)-trien-17-yl] ethylmethyl-(9CI).

Hypersensitive response (HR) is the most eminent and effective innate defense system in plants, characterized by the rapid programed cell death around the infection/feeding sites. It has long been proposed in the research field of nematology that HR is developed upon and limits the establishment and spread of PPN infections. However, our real-time ‘live’ imaging between RN

and cotton lines of tolerant, hypersensitive and susceptible phenotypes has failed to corroborate the old hypothesis. Instead, we observed that the tolerance line developed significant increased numbers of root hairs compared to hypersensitive and susceptible lines, suggesting that root growth and/or root hair development are related to plant tolerance against PPN infections. Moving forward, we have employed a system biology approach to discern i) the tolerance associated genes and ii) if those genes are involved in root morphology by analyzing differential transcriptomes between the tolerant and susceptible cotton lines before and after nematode infections.

AKNOWLEDGEMENTS

I thank my advisor, Dr. Sang-Wook Park for his constant encouragement, support and direction during my studies. His insights and mentoring have been invaluable to the past two years. I would like to thank Dr. John Murphy and Dr. Aaron Rashotte for their time, and the many helpful suggestions and recommendations as members of my thesis committee. I would like to thank Dr. Victoria Owens and Dr. Robert Locy for their willingness to collaborate on specific topics of my thesis. I would like to thank my co-workers, Ross Jeffery, Izaila Barbosa dos Santos, Wenshan Lui, Anne Moye and Alexis Jones for their support and friendship.

I would like to thank my parents for instilling the principles of hard work and independent thought in me, and for encouraging me to pursue higher education. I would like to thank my siblings for their support and being my obligatory lifelong best friends. I would most of all like to thank my Auburn and Minnesota friends for their continuing love, support and memes from near and far. I would like to thank someone special for cooking multiple meals, continuously encouraging me, and for always having my back. You know who you are. And finally, I thank myself. Through the tears of stress and the smiles of bliss, you did it. I am so proud of you for this accomplishment and excited for what the future holds.

LIST OF FIGURES

TABLE OF CONTENTS

CHAPTER 1: INTRODUCTION AND REVIEW OF LITERATURE

1.1 INTRODUCTION AND PROBLEM STATEMENT

Cotton is the leading fiber cash crop of the world playing a large role in everyday lives, from job stability to everyday comfort. However, this crop suffers from an endless cycle of diseases and damages from different pathogens, one being parasitic phytonematodes. These microscopic roundworms develop an obligate parasitic relationship with plant hosts that can have negative effects on crop growth and yields. Once to the root surface, phytonematodes insert a stylet, a needle-like structure, and feed cytosolic nutrients from roots, which can affect root cell tissues negatively (Mitchum et al. 2013, Fous-Nyarko and Jones 2016). In the modern agriculture, phytonematodes do not cause specific disease or death of entire plants per se, but like herbivore feeding, they can damage crop's root system and reduce plant's ability to absorb water and nutrients (Lambert 2002). Typical phytonematode damage symptoms are a reduction in root mass, a distortion of root structure, root stunting. Nematode damage of plant's root system most importantly, provides an opportunity for other plant pathogens to invade roots, thus further weakening plant (Lambert 2002). Phytonematodes and their related damages have become of great economic importance causing an estimated annual loss of 10 percent of world crop production (Nicol et al. 2011), thus needing an urgent breakthrough in developing effective and sustainable disease management programs such as new resistance cultivars. It is however not necessarily forthcoming, largely due to our little knowledge of the pathophysiology of phytonematodes and plant defense responses against them.

As an initial step to understand the modes of defense responses in plant (e.g. cotton) roots towards phytonematode infections, hypersensitive response (HR) was investigated. HR plays a critical role in plant innate immunity whereby host R-genes will recognize effector proteins

derived from pathogens and respond by programmed cell death within a small perimeter of the infection sites, thus preventing spread of biotrophic pathogens. Although proposed for decades, no data clearly shows phytonematodes causing HR in plant (e.g., cotton) roots. As of now, plant-phytonematode interactions are regarded as direct host-pathogen interactions, due to the knowledge of *Mi-1* gene (referred as R-gene) conferring resistance to phytonematodes (Vos 1998). To understand and validate HR activity when cotton is under phytonematode invasion, real-time imaging analyses via confocal microscopy was used. Interactions of RN to three different cotton germplasms were then observed and analyzed. The tolerant germplasm, Barbren-713 was used based on its performance in RN resistance and promising agronomic potential (Bell 2015). Hypersensitive germplasm, Lonren-1, was predicated to display HR with decreased infection. SG-474 germplasm was used as the susceptible line. While developing preliminary data, roots were stained with propidium iodide (PI) solution to visualize membranes under the TRITC (Tetramethylodamine, red) filter. The FITC (fluorescein isothiocyanate, green) channel was viewed to clarify chloroplast was not present, and with a serendipitous find, the phytonematodes autofluoresced. Further characterization and identification testing was done. Though, our real-time imaging analyses unveiled that no HR is developed in cotton roots upon phytonematode infections, inferring that a canonical R-gene is not crucial in root defense mechanism against phytonematodes. Instead, our study suggests the importance of root hair growth and/or root development. Together, our results re-recognize plant-phytonematode interactions as plant-insect/herbivore interactions rather than plant-microbe interactions.

As alluded, it was observed that phytonematodes constitutively produced autofluorescent compounds throughout their life spans, implying this metabolite is intrinsic. Thus, the present study employed an analytical high-performance liquid chromatography (HPLC), and liquid

chromatography-mass spectrometry (LC-MS) to identify the compound. The RN-derived autofluorescent compound is eluded throughout polar (or nonpolar) fractions in a water to methanol column, and which produce masses of something. These masses were collected how and assembled how, generating a Sulfonium, [(17β) -3-ethoxyestra-1,3,5(10)-trien-17-yl]ethylmethyl-(9CI).

Moving forward, we have employed a system biology approach to discern **i**) the tolerance associated genes and **ii**) if those genes are involved in root morphology by analyzing differential transcriptomes between the tolerant and susceptible germplasms before and after nematode infections. As an initial step level differences of transcripts between tolerant (Barbren-713, Bar0) and susceptible (SG-747, DSO), and hypersensitive (Lonren-1, L10) germplasms were established via the National Center for Biotechnology Information (NCBI) database and Blast2GO software. Since most of genes found in the results of DSO v. L10 are likely irrelevant (or negative) to tolerance phenotype, we are now subtracting those genes from the results of DSO v. Bar0. In addition, we have been generating a comprehensive list of genes related to root growth and root hair development based on *Arabidopsis* database and identifying their homologues in cotton plants and analyzing their expression levels in Bar0 compared to DSO and L10.

Molecular function GO annotations between SG-747 susceptible (DSO) germplasm and Barbren-713 tolerant (Bar0) germplasm had the most differentially expressed transcripts of ATP binding, nucleotide binding and hydrolase binding. Biological process GO annotations between the two have differentially expressed transcripts of oxidation-reduction process, phosphorylation and transmembrane transport. Molecular function GO annotations between SG-747 susceptible (DSO) germplasm and Lonren-1 hypersensitive (L10) germplasm have the most differentially

expressed transcripts of ATP binding, metal ion binding and DNA binding. Biological process GO annotations in the same two are translation, transmembrane transport and defense response.

Together, the present study results are that natural autofluorescent material identified as a Sulfonium, [(17β) -3-ethoxyestra-1,3,5(10)-trien-17-yl]ethylmethyl-(9CI) in the RN intestinal system. RN auto fluorescence tested to be stable under multiple stressful pH, DTT and H_2O_2 conditions and possess a unique excitation of 425 nm and emission of 525 nm. Real-time imaging analysis unveiled no HR is developed in cotton roots upon RN infections, inferring that canonical R-gene is not crucial in root defense mechanism against phytonematodes. Among the most differentially expressed genes, we are digging deeper to find root related genes that are differentially regulated between tolerance verses susceptible germplasms.

1.2 HISTORIC ROLES AND IMPORTANCE OF COTTON AGRICULURE AND THE RECENT EMERGENCE OF PEST ATTACKS

Since its domestication, cotton has played major roles socially and economically in the history, especially in the U.S., leading the westward expansion, industrial revolution and the Civil War (Martin 1994). Today, cotton farming in the U.S. accounts for about one quarter of the world supply (Koenning 2004), producing 17 million bales annually (~$25 billion), and creating over 200,000 jobs (NCCA 2013). Processing and handling cotton after it leaves the farm generates even more business activities and revenues (Cotton Counts 2017). The entire cotton plant is used and valued in different industries. The fiber is developed into cloth and linters, while the short fuzz on the seed provides cellulose for the productions of plastics, explosives, high quality papers, and furniture and automobile cushions. The cottonseed is crushed for oils, and the mill and hull remaining is used for livestock feed (Tyson 2015).

Cotton, like any other economically important crop, undergoes biotic and abiotic stresses that hinder agronomic sustainability of cotton agriculture. Phytonematode-induced microbial pathogen diseases and damages, result in reduced growth and yields, causing the loss of millions of dollars. Especially, phytonematodes have lately emerged as major threats to cotton growing across the world. (Thiessen 2018). The most damaging phytonematodes to cotton include root knot nematode (*Meloidogyne spp*.), soybean cyst nematode *(Heterodera glycines)* and reniform nematode (*Rotylenchulus reniformus*) (Sasser 1972), which have been causing significant delay in maturity, and reductions in the yield of cotton lint and the size of bolls (Jones 1958). *R. reniforms* have lately become a major threat over the last decade towards cotton farming in the southern regions of the U.S., leading to an estimated yield loss of over $100 million annually. Cotton is the most important fiber producing crop of which its production in the U.S. accounts for about one quarter of the world supply (~ $25 billion values, Koenning et al. 2004,), and creates over 200,000 jobs (NCCA 2015). However, the currently available integrated pest management method against phytonematodes (IPM-P) is limited to the casual application of toxic pesticides, which in turn has caused numerous unexpected ecological, economic and social drawbacks. Hence to develop more efficacious and sustainable IPM-P, many efforts have made over the past 10 years to understand the pathophysiology of plant-phytonematode interactions, but our knowledge regarding *i*) the pathogenicity of phytonematodes and *ii*) the defense responses of host plants against phytonematodes are still rudimentary, compared to other plant-microbial pathogen interactions.

Common symptoms in cotton plants caused by parasitic phytonematodes include stunting, yellowed leaves and wilting. Once symptoms occur, the current season's crop has a difficult time recovering if phytonematodes are not managed. If not, other pathogens, such as bacteria or fungi, have an increased opportunity to infect, causing further damages and possibly serious disease.

The susceptible cotton germplasm Sure-Grow 747 (SG-747) is used in various studies being bred with other stains to create F2 generations of with desired traits (McCarty 2017). The Upland cotton germplasm Barbren-713 was developed and released by the USDA-ARS, Mississippi Agricultural and Forestry Experiment Station, Texas A&M AgriLife Research and Cotton Incorportated in 2012. The germplasm was designed for private and public breeders to sustain high resistance to both RN and root-knot nematodes. The source of resistance to RN associated primarily with Ren_2^{GB713} gene on chromosome 21 were derived from *G. basbadense* cultivar (TX 110) GB713, which has been reported to delay RN infection and development (Robinson, et al., 2004, Stetina 2015). Resistance to root-knot nematode was transferred from the germplasm line M-315 RNR (PI 592514) and is associated primarily with the dominant Mi-1 gene and the additive Mi-2 gene on chromosome 11 (McPherson et al., 2004). In controlled environment assays, both nematodes were reproductively suppressed by 90% or more (Bell et al., 2015).

The Upland cotton (*Gossypium hirsutum L.)* germplasm line Lonren-1 was developed and released by the USDA-ARS, Texas Agricultural Experiment Station and Cotton Incorporated in 2007, providing breeders with a resistant germplasm to RN. In 1984, it was found that the wild species *G. longicalyx* from East Africa was immune to RN, failing to support any continuous RN reproduction (Yik and Birchfield 1984). To develop a resilient germplasm, resistance was transferred from *G. longicalyx* ($2n = 2x = 26$) to *G. hirsutum* ($2n = 4x = 52$, genome designation AD_1). Introgression of genes from the unique diploid F_1 genome of *G. longicalyx* into either the A or D subgenome of the triple-species hybrid, referred to as HLA (*hirsutum-longicalyx-armourianum*). HLA is expressed with a high level of resistance to RN and was has been used as a bridging hybrid in a backcross breeding program (Bell and Robinson, 2004). HLA has the complete sets of all three-cotton species in its makeup (Bell et al. 2014). Lonren-1 and another

line, Lonren-2, were derived using crosses and backcrosses into *G. hirsutum* cultivars, based on bioassays of 10 single-seed descendants for resistance to RN and agronomic performance.

1.3 *ROTYLENCHULUS RENIFORMIS* BIOLOGY

Plant parasitic nematodes, belonging to the phylum *Nematoda*, are microscopic animals that have evolved to over 4,000 species and have adapted to a broad range of environment from forests to oceans (Nicol et al. 2011, Hodda 2011, Zhang 2013). Previously, many - if not most - of them were viewed as benign or non-damaging, but several recent reports have recognized that selective species such as *Rotylenchus* spp. *Meloidogyne* spp. and *Heterodera* spp., are agronomical important pests, attributing the annual losses of crop production at ~10 % worldwide (Nicol 2002, Nicol et al. 2011). In the past decade, RN has become of significance in the state of Alabama, for each year, infestations in crops increase.

Reniform nematodes are sedentary semi-endoparasites that partially penetrate a wide variety of plants. The term reniform refers to the kidney-shaped body of a mature female. RN, unlike root-knot or cyst nematodes, require plant roots to survive and reproduce (Lambert 2009). The head of RN penetrates the root cortex and uses the stylet to puncture root cells to form a permanent feeding cell. The RN tail region (posterior portion) protrudes from the root and swells during maturation (Wang 2007). After swelling, RN do not move once they have entered the endoparasitic phase of their life cycle. By giving up mobility, RN risks death if their host plant dies, but they also benefit from their feeding site, having an abundance of nutrient uptake and reproductive potential.

RN was first reported to be found on cowpea roots in Hawaii (Linford and Oliveira 1940) but was unknowingly transported to the state of Georgia in the southern U.S. where they were

introduced to cotton (Koenning 2004). Now, RN is distributed in tropical, subtropical and warm temperate zones throughout the southern U.S. (Ayala and Ramirez 1964). Along with cotton, RN target more than 300 other plants species (Robinson et al. 1997).

In every phytonematode life cycle, eggs hatch one to two weeks after being laid where the first stage juvenile molts within the egg, producing second-stage juvenile (J2) that emerges from the egg. Female nematodes at the J2 developmental period are highly infective and will opportunistically penetrate any area of the root system. Males remain outside the root and can inseminate a female before she is matured. Soon after female gonad maturation, the eggs are fertilized with sperm, and about 60-200 eggs are deposited into a gelatinous matrix (Wang 2007). Some species of nematodes reproduce parthenogenetically (egg production without fertilization). Nematode life cycles last about three weeks depending on temperature, though, nematodes can survive at least two years in the absence of a host in dry soil through anhydrobiosis, a survival mechanism which allows the nematode to enter an ametabolic state and live without water for extended time periods (Radwald and Takeshita 1964).

1.4 CURRENT KNOWLEDGE OF AUTOFLUORESCENE IN PHYTONEMATODES

RN among other phytonematodes have been observed to autofluorescence naturally, yet little information is known about whether it is related to *Caenorhabditis elegans* aging autofluorescence. Autofluorescence is the natural emission of light by biological structures such as mitochondria and lysosomes when they have absorbed light and is used to distinguish the light originating from artificially added fluorescent markers (fluorophores) (Lam 2013). Many areas of nematology research require the ability to distinguish live from dead nematodes. Mobility, spontaneous or induced, is an obvious form of viability, yet, the lack there of, does not indicate

that the nematode is dead. This distinction is particularly important in research on population dynamics and pesticide efficacy (Forge 1989). Using stains as a form of viability has been used but is not effective in distinguishing live from dead nematodes (Bird 1979, Chadhouri 1966). Stains work only if the event of inducing death results in cuticle permeability (Hollis 1961). Consequently, the reliability of any stain is affected by inducing mortality with the harshness of the event and the length of time between death and staining. Characterizing phytonematode autofluorescence can be beneficial for live observation research, since staining can be detrimental in viability, skewing results.

Autofluorescent material described in *C. elegans* (Hannover 1842), is described as lipofuscin, an age-pigment, and has been characterized in other organisms including deep sea invertebrates (Jung 2007, Terman 2004, Brunk 2002, Yin 1996). Many bacteria, actinomycetes, algae, and fungi also autofluoresce naturally; and the presence of invading organisms, especially actinomycetes, has been detected clinically, as well as in plants and animals, by this method (e.g. invasion of potato by *Streptomyces scabies)* (Darken 1960). Lipofuscin are composed of lipid-containing residues of lysosomal digestion, have a yellow-brown pigment, autofluoresce yellow when excited by ultraviolet light and accumulate during normal senescence (Katz 2002) Lipofuscin in *C. elegans,* builds up over its lifetime within intestinal cell tissue with low turnover, increases with age and with oxidative damage and is commonly used as a marker of cellular aging studies (Terman 2006). The exact relationship between autofluorescence, aging, and lifespan in *C. elegans* has remained somewhat ill defined. However, different groups of researchers have come to different conclusions whether autofluorescence wavelengths do (Gerstbrein 2005, Pincus 2011) or do not (Coburn 2013, Sánchez-Blanco 2011) determine overall health of an individual or population of animals. For example, Bird Notwithstanding, studies use accumulation of intestinal

autofluorescence in *C. elegans* to measure whether interventions improve health or slow aging (Pincus 2016).

1.5 PLANT DEFENSE RESPONSES TO PHYTONEMATODES

The current working model of plant-nematode interactions is built based on the hypothesis that plant roots operate essentially similar - if not the same - defense mechanisms against phytonematodes as do plant leaves against other microbial and herbivore pathogens. Unlike animals, plants do not have a specialized adaptive immune system that recognizes, directly attacks and destroys infectious agents. Instead, plants are endowed with a broad range of sophisticated and efficient innate immunity mechanisms that enable them to recognize and restrain a plethora of pathogenic microbes in their natural habitat (Jones and Dangl, 2006). Indeed, a single dominant gene (*Mi-1*) conferring resistance against the root-knot nematode *Meloidogyne* spp. was isolated over half a century ago from a tomato relative (*Lycopersicon peruvianum*, Bailey 1941). Since then, the major research goals of plant-nematode interactions have focused on espying phytonematode-derived avirulence (*avr*)-genes (also called effectors) that bind and trigger resistance (*R*)-gene (e. g. *Mi-1*)-mediated resistance (also called effector-triggered immunity, ETI). However, the identity of phytonematode-dirived *avr*-gene is - if it is present - still elusive. Instead, several studies have proposed a pivotal role of phytonematode-derived cell wall degrading enzymes (CWDE, sugar hydrolases) in host plant defense responses, although their modes of action are not yet understood (Mitchum et al. 2013, Fosu-Nyarko and Jones 2016). On the other hand, a recent study has underpinned that phytonematodes secrete conserved molecules, so called ascarosides that are capable of eliciting PAMP (pathogen-associated molecular pattern) responses (referred to PAMP-triggered immunity, PTI, or basal resistance) in various plants (Manosalva et

al. 2015). Although the cognate pattern recognition receptors (PRRs) of ascarosides are yet to be identified, this finding reveals the perception of PAMPs and other molecular patterns converges on triggering plant immunity. In addition, these results perhaps shed new light on an actual role of phytonematode-derived CWDE, which could activate the production of damage-associated molecular patterns (DAMP), despite of targeting to nucleotide binding domain leucine rich repeat protein (NB-LRRs) leading to ETI, in inducing several downstream signaling events during plant immune responses (Gillet 2017).

It has long been proposed that hypersensitive response transpires in cells located near invading phytonematodes (Rice et al. 1985). A general definition of hypersensitive response is an area of cell death that forms at the point of attempted pathogen ingress and which correlates with the exhibition of resistance (Mur 2008). Microscopic imaging observed a layer of necrotic cells at the periphery of syncytium produced upon phytonematode infection, and those cell deaths were greater in resistant vs. susceptible potato lines although the reactions were comparatively slower than the typical HR. Since then, several studies have frequently monitored similar, if not same, HR-like responses in various plant cells towards phytonematode infections (Anthony *et al*. 2005, Agudelo *et al*. 2005, Khallouk *et al*. 2011, Cabasan *et al.* 2014) in parallel with accumulations of reactive oxygen species (ROS) and phenolic compounds, classic chemical signals of HR (Waetzig et al. 1999, Pegard et al. 2004, Melillo et al. 2006, 2011, Simmonetti et al. 2009). However, it is still unclear whether this HR-like phenomenon observed during phytonematode infections is a) an example of programmed cell death (PCD) or cell lysis, or b) correlated with root resistance towards PPN (Williamson and Kumar 2006), especially considering that i) ROS productions are not prerequisite of HR, instead could suppress cell death responses while promoting pytonematode infections (Siddique et al. 2014), as well as most if not all histological analyses conducted thus far

ii) employed extensive fixation processes which potentially cause the physical and/or physiological alteration of cells (Santana et al. 2015), and iii) monitored HR-like responses at >3 d post phytonematode inoculations. The later, rather slower than the typical foliar HR (Rice et al. 1985, Mur et al. 2008), implies that PPN-induced root HR may be physiologically and biochemically unique, or perhaps less effective. Alternatively, those cell deaths seen along with PPN infections are not PCD but physical damages.

1.6 ROOT MORPHOLOGY AND ROOT HAIRS

Cotton develop a complex root system. Cotton roots consist of a primary or 'tap' root which grow for several days after germination without branching (McMichael 1993). When cotton is planted in a field, when branching occurs, the lateral root primordia develop generally about 12 cm behind the primary root apex with tertiary roots developing about 5 cm behind the secondary root apex (Mauney 1968). If the primary root is injured, there generally is an increase in the number of secondary roots one of which may take over and act as the primary root (McMichael 1993). Among secondary and tertiary roots are much smaller roots called root hairs. Root hairs are long tubular-shaped outgrowths from the epidermal cells of the roots that have many characteristics (Grierson 2002). They vastly increase root surface area, enhancing nutrient and water uptakes and help to anchor the plant in the soil (Bibikova 2002). Root hair development provides insight into a range of developmental processes from cell fate determination to growth control. Root hair development occurs in a series of processes starting with cell fate specification in the meristem. The epidermal cell that forms the root hair, or trichoblast, contributes in the diffuse growth phase associated with the elongation of the primary root axis. When elongated trichoblast exits the elongation zone, growth is reorganized, and root hair initiation begins. Initiation is followed by a

sustained phase of tip growth until the hair reaches its mature length (Bibikova 2002).

In our studies, it was observed that the amount of root hair growth also depends on germplasm, whether healthy or interacting with pytonematodes. Understanding that root hairs play many roles to benefit the plant can help decipher plant physiology when under stress.

1.7 LITERATURE CITED

Agudelo, P., R. T. Robbins, J. M. Stewart, A. Bell, and A.F. Robinson. 2005. Histological observations of Rotylenchulus reniformis on Gossypium longicalyx and interspecific hybrids. J. Nematol. 37:444–447.

Ayala A., C.T. Ramirez.1964. Host-range, distribution, and bibliography of the reniform nematode, *Rotylenchulus reniformis*, with special reference to Puerto Rico. Journal of Agriculture of University of Puerto Rico 48: 140-160.

Bailey, D. M. 1941. The seedling method for root-knot nematode resistance. Proc. Am. Hort. Sci. 38: 573-575.

Bell, A.A., and A.F. Robinson. 2004. Development and characteristics of tri-species hybrids used to transfer reniform nematode resistance from *Gossypium longicalyx* to *Gossypium hirsutum*. In: Proceedings of the Beltwide Cotton Conferences, San Antonio, TX. 5–9

Bell, A.A., and A.F. Robinson. 2014. Registration of LONREN-1 and LONREN-2 germplasm lines of upland cotton resistant to reniform nematode. Journal of plant registration doi: 10.3198/jpr2013.11.0069crg.

Bell, A.A., et al. 2015. Registration of BARBREN-713 germplasm line of upland cotton resistant to reniform and root-knot nematodes. Journal of Plant Registrations 9:89-93.

Bird, A. F. 1979. A method of distinguishing between living and dead nematodes by enzymatically induced fluorescence. Journal of Nematology 11:103- 105.

Bibikova, T., T. Gilroy. 2002. Root hair development. Journal of Plant Growth Regulation 2: 383-415.

Biology Discussion. 2017. (http://www.biologydiscussion.com/plants/plant-diseases/diseases-of-cotton-plant-diseases/43125) (Obtained November 15, 2017).

Brunk U. T., A. Terman. 2002. Lipofuscin: mechanisms of age-related accumulation and influence on cell function. Free Radic Biol Med. 33:611–619.

Chadhouri, N., R. I. Dick, R. S. Englebrecht, and J. H. Austin. 1966. Staining of free-living nematodes by eosin-y dye. Nematologica 12:337-342.

Cotton Counts. 2017. (https://www.cotton.org/pubs/cottoncounts/story/importance.cfm) (Obtained November 15, 2017).

Coburn C, et al. 2013. Anthranilate fluorescence marks a calcium-propagated necrotic wave that promotes organismal death in *C. elegans*. PLoS Biol. 11:e1001613.

Curtis, R. H. C. 2008. Plant-nematode interactions: environmental signals detected by the nematode's chemosensory organs control changes in the surface cuticle and behaviours. Parasite 15: 310-316.

Datta, S., C. M. Kim., M. Pernas, N. D. Pires, H. Proust, T. Tam, P. Vijayakumar, L. Dolan. 2011. Root hairs: development, growth and evolution at the plant-soil interface. Plant and Soil 346 (1-2):1-14.

Forge, T. A. and MacGuidwin, A. E. 1989. Nematode autofluorescence and its use as an indicator of viability. Journal of nematology 21(3): 399-403.

Fosu-Nyarko J, M. G. K Jones. 2016. Advances in understanding the molecular mechanisms of root lesion nematode host interactions. Annu Rev Phytopathol 54: 253-278.

Gerstbrein B., G.Stamatas, N. Kollias, M. Driscoll. 2005. In vivo spectrofluorimetry reveals endogenous biomarkers that report healthspan and dietary restriction in *Caenorhabditis elegans*. Aging Cell. 4:127–137.

Gillet, F. X., C. Bournaud, J. D. A. de Souza Júnor, M. R. Grossi-de-Sa. 2017. Plant-parasitic nematodes: towards understanding molecular players in stress responses. Ann Bot 119: 775-789.

Grierson, Claire and J. Schiefelbein. 2002. Root Hairs. American Society of Plant Biologists 1: e0060.

Hannover A. 1842. Mikroskopishe Undersogelser af Nevensystem. Natrurv. Math. Ajh. Copenhagen. 10:1–112.

Hodda. M. 2011. Phylum Nematoda Cobb, 1932, In: Zhang ZQ (eds) Animal Biodiversity: An Outline of Higher-level Classification and Survey of Taxonomic Richness. Zootaxa 3148: 63-95.

Hollis, J. P. 1961. Nematode reactions to coal tar dyes. Nematologica 6:315-325.

Jung T., N. Bader, T. Grune. 2007. Lipofuscin: formation, distribution, and metabolic consequences. Ann N Y Academy of Science 1119: 97–111.

Jones, J. E., L. D. Newson., and E. L. Finley. 1958. Effect of Reniform nematode on yield, plant character, and fiber properties of upland cotton. American Society of Agronomy. 51: 353-356.

Jones J.D.G. and J. L. Dangl. 2006. The plant immune system. Nature 444:323-329.

Katz, M. L. and W. G. Robinson. 2002. What is lipofuscin? Defining characteristics and differentiation from other autofluorescent lysosomal storage bodies. Archives of gerontology and geriatrics 34(3): 169-84.

Koenning, S.R., J. A. Wrather, T. L. Kirkpatrick, N. R.Walker, J. L. Starr, J. D. Mueller. 2004. Plant-parasitic nematodes attacking cotton in the United States: Old and emerging production challenges. Plant Dis 88: 100-113.

Lambert, K. and S. Bekal. 2002. Introduction to lant-Parasitic Nematodes. *The Plant Health Instructor*. DOI: 10.1094/PHI-I-2002-1218-01

Lam, L. A. Learn more about autofluorescence angioid streaks. Elsevier, Retina (Fifth Edition). 2: 1267-1273.

Linford M. B., J. M. Oliveira. 1940. *Rotylenchulus reniformis*, nov. gen. n. sp., a nematode parasite of roots. Proceeding of the Helminthological Society of Washington 7: 35-42.

Manosalva, P., M. Manohar, S. H. von Reuss, S. Chen, A. Koch, F., Kaplan, A. Choe, R. J. Micikas, X. Wang, K. H. Kogel, P. W. Sternberg, V. M. Williamson, F. C. Schroeder, D. F. Klessig. 2014. Conserved nematode signaling molecules elicit plant defenses and pathogen resistance. Nat Commun 6: 7795.

Martin, S. B., et al. 1994. A survey of South Carolina cotton fields for plant-parasitic nematodes. Plant Dis. 79:717-719.

McCarty, J. C. Jr. et al. 2017 Registration of six germplasm lines of cotton with resistance to the root-knot and reniform nematodes. Journal of Plan Registrations 11(2). 10.3198/jpr2016.09.0044crg.

McPherson, M. G., J. N. Jenkins, C. E., Watson, and J. C. McCarty. 2004. Inheritance of root-knot nematode resistance in M315 RNR and M78 RNR cotton. J. Cotton Sci. 8:154–161

Mitchum, M. G., R. S. Hussey, T. J. Baum, X. Wang, A. A., Elling, M. Wubben. E. L. Davis, 2013. Nematode effector proteins: an emerging paradigm of parasitism. New Phytol 199: 879-894.

Mur, L. A. J., P. Kenton, A. J. Lloyd, H. Oughum, E. Prats. 2008. The hypersenstive response; the centenary is upon us but how much do we know? 59 (3): 501-520.

National Cotton Council of America (NCCA). 2015. NCC Comments on Pollinator Proposal. Available at http://www.cotton.org/issues/2015/polcomm.cfm.

Nicol, J. M. 2002. Important nematode pests, In: Curtis, B. C., Rajaram, S., Gómez, M. (eds) *Bread sheat improvement and production*. FAO Plant production and Protection Series, p 567.

Nicol, J. M., S. J. Turner, D. L. Coyne, L. den Nijs, S. Hockland, Z. Tahna Maafi. 2011. Current nematode threats to world agriculture, In: Jones, J., Gheysen, G., Fenoll, C. (eds), *Genomics and Molecular Genetics of Plant-Nematode Interaction*. Springer, Germany, pp 21-43.

Pincus, Z., T. C. Mazer, F. J. Slack. 2016. Auto fluorescence as a measure of senescence in C. elegans: look to red, not blue or green. Aging 8(5): 889-898.

Radewald J. D., G. Takeshita. 1964. Desiccation studies on five species of plant-parasitic nematodes of Hawaii. Phytopathology 54: 903-904.

Robinson, A. F., A. C. Bridges, and A. E. Percival. 2004. New sources of resistance to the reniform (*Rotylenchulus reniformis* Linford and Oliveira) and root-knot [*Meloidogyne incognita* (Kofoid and White) Chitwood] nematode in upland (Gossypium hirsutum L.) and sea island (G. barbadense L.) cotton. J. Cotton Sci. 8:191–197.

Sasser, J. M. 1972. Nematode diseases of cotton. Dept. of Plant Pathology, North Carolina State Univ., Raleigh, North Carolina, USA. Economic nematology: 187-214 pp.

Sikkens, R. B., D. B. Weaver, K. S. Lawrence, S. R. Moore, and E. van Santen. 2011. LONREN upland cotton germplasm response to Rotylenchulus reniformis inoculum level. Nematropica 41:68–74.

Stetina, S. R. 2015. Postinfection development of *Rotylenchulus reniformis* on resistance *Gossyium barbadense* accessions. Journal of Nematology 47(4): 302-309.

Terman A, U. T. Brunk. 2004. Lipofuscin. Int J Biochem Cell Biol. 36:1400–1404.

Terman A, U. T. Brunk. 2006. Oxidative stress, accumulation of biological 'garbage', and aging. Antioxid Redox Signal. 8:197–204.

Thiessen, L. 2018. Disease Management in cotton. Department of Crop and Soil Sciences: Cotton Information. NC State University.

Tyson, Luna. 2015. Importance of Cotton. (http://offices.aces.edu/montgomery/importance-of-cotton/) (Obtained November 15, 2017).

Wang, Koon-Hui. 2007. Featured Creatures: Reniform nematodes. University of Florida. (http://entnemdept.ufl.edu/creatures/nematode/r_reniformis.htm) (Obtained November 17, 2017).

Yik, C. P. and W. Birchfield. 1984. Resistant germplasm in Gossypium species and related plants to Rotylenchulus reniformis. J. Nematol. 16: 146-153.

Yin D.Z., U. T. Brunk. 1991. Microfluorometric and fluorometric lipofuscin spectral discrepancies: a concentration-dependent metachromatic effect? Mech Ageing Dev. 59:95–109.

Zhang, Z. 2013. Animal biodiversity: An update of classification and diversity in 2013, In: Zhang, Z. Q. (eds) Animal Biodiversity: An Outline of Higher-level Classification and Survey of Taxonomic Richness (Addenda 2013). Zootaxa 3703: 5-11.

Zhou, E., and J. L. Starr. 2003. A comparison of the damage functions, root galling, and reproduction of Meloidogyne incognita on resistant and susceptible cotton cultivars. J. Cotton Sci. 7:224–230.

CHAPTER 2*:* IDENTIFICATION AND CHARACTERIZATION OF AUTOFLUORESCENCE COMPOUND FROM *ROTYLENCHULUS RENIFORMIS*

1.8 ABSTRACT

Plant parasitic reniform nematodes (*Rotylenchulus reniformis*, RN) are of significant economic importance worldwide. In the U.S., cotton is a major host crop of RN, causing considerable yield suppression via nutrition deprival, fruit abortion and abnormal maturation (Koenning 2004). Thus, an urgent breakthrough is needed in understanding the pathology of phytonematode infections and development of effective and sustainable pest management programs, including new resistant cultivars of cotton. Therefore, our studies have focused on investigating the mechanisms of innate defense responses (e.g., hypersensitive response, HR) in cotton roots (reviewed in Chapter 3). Thereby, we have serendipitously discovered a natural autofluorescent material, accumulated in the intestinal system of RN. The excitation and emission length proved that the green signal of RN-derived autofluorescent material is unique, different from both a commonly known green fluorescent protein (GFP) of jellyfish (Chalfie 1995) and a green age-related pigment, namely lipofuscin, of *Caenorhabditis elegans* (Pincus 2016). Therefore, identification and functional characterization of this mystery molecule will help us **a**) better understand the basic physics of fluorescent chemistry, **b**) further uncover cellular metabolites and mechanisms of phytonematode biology, and **c**) evaluate its potential values and applicability, especially since the RN-derived autofluorescence was tested to be considerably insensitive to light and stable under multiple stress conditions (extreme high or low pH and H_2O_2). We thus employed high performance liquid chromatography (HPLC), liquid chromatography-mass spectrum (LC-MS), and nuclear magnetic resonance (NMR) to identify and determine a

chemical identity. To this end, proton assembly of the RN-derived autofluorescent compound depicted to be Sulfonium, [(17β) -3-ethoxyestra-1, 3,5(10)-trien-17-yl]ethylmethyl-(9CI).

1.9 INTRODUCTION

Plant parasitic nematodes (PPN) are of great economic importance in agriculture across the world, causing significant yield losses of various commercially important crops. In the southern U.S., the infestations of PPN attribute the annual losses of cotton productions at estimated 10 % (Nicol *et al.* 2011). Indeed, roughly $35 million worth of cotton yields are lost (Gazaway 2007) by one species of PPN, *R. reniformis* (RN), in the state of Alabama alone. Therefore, pest management programs have focused on developing tolerant or fully resistant cotton cultivars against PPN infections. Developing new cultivars however have proven to be very difficult, especially due to a narrow genetic diversity of cotton germplasms, and little understanding of their genetic principles associated with defense responses against PPN.

To investigate the pathophysiology of cotton-PPN interactions, we aimed at developing a real-time visualization technique using conformal microscopy and non-toxic fluorescent dyes such as propidium iodide and 2',7'-dichlorofluorescein to capture RN infection processes towards cotton roots. In an initial optimization step of the imaging protocol, we serendipitously discovered that RN internally accumulated an autofluorescent substance, emitting stable signals via the green channel. Thus, we decided to explore the chemical identity and nature of the RN-derived autofluorescent compound as little information is available for autofluorescence in PPN biology.

Green fluorescent protein (GFP) derived from jellyfish is widely used for academic and clinical research (Chalfie 1995). Autofluorescent material transpires when a fraction of light illuminating an object is absorbed and then re-emitted as a different color (Terman and Brunk,

2006). It is generally used as a tag or a probe to stain targeted materials, tissues, or cells for all areas of science, both basic and applied. The quality of materials and at what excitation and color they fluoresce, characterizes auto fluorescence differently. In *C. elegans*, red fluorescent signals correlate with live tissue health, whereas blue fluorescent signals indicate dead cells. On the other hand, green fluorescent signals can be a combination of living and dying materials, depending on species (Pincus *et al*. 2016). However, nematodes lost fluorescence signals when there were killed by excessive heat, freezing and formaldehyde application, demonstrating that the fluorescence is an indication of viability (Forge and MacGuidwin 1989).

The objectives for the present studies are **1**) to characterize the chemical nature, **2**) to identify the chemical structure of RN-derived autofluorescent substance, and **3**) to its roles and functions in the pathophysiology of PPN during their interactions with host plant roots, which in turn benefit understanding of basic physiology, and development of new pest management tools of PPN infected cotton.

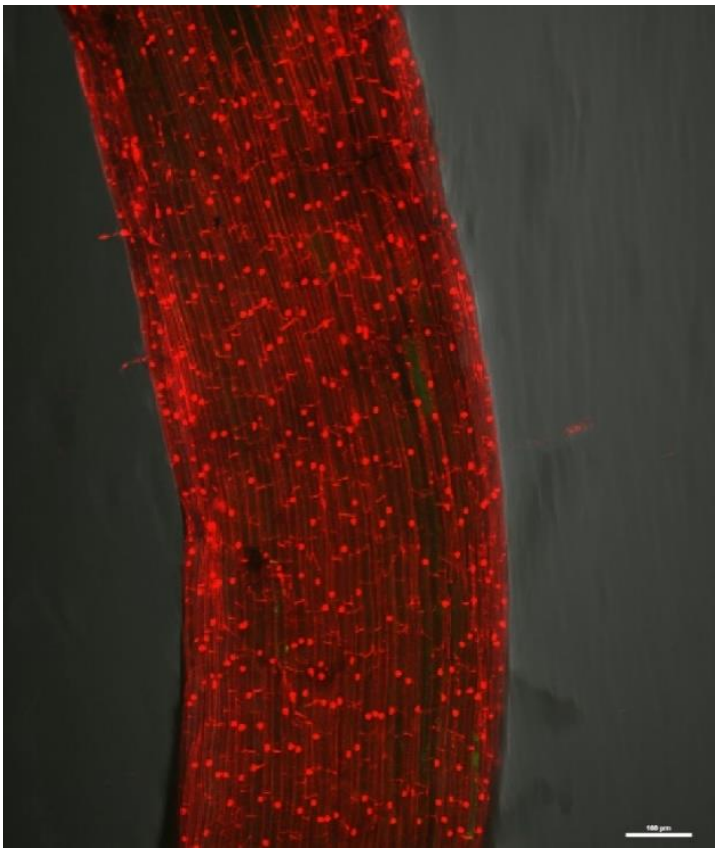

Figure 1: Example of secondary root stained with PI stain. To visualize cotton roots against RN, propidium iodide stain is used to visualize the individual cell membranes (lines) and nuclei (dots) using confocal microscopy imaging.

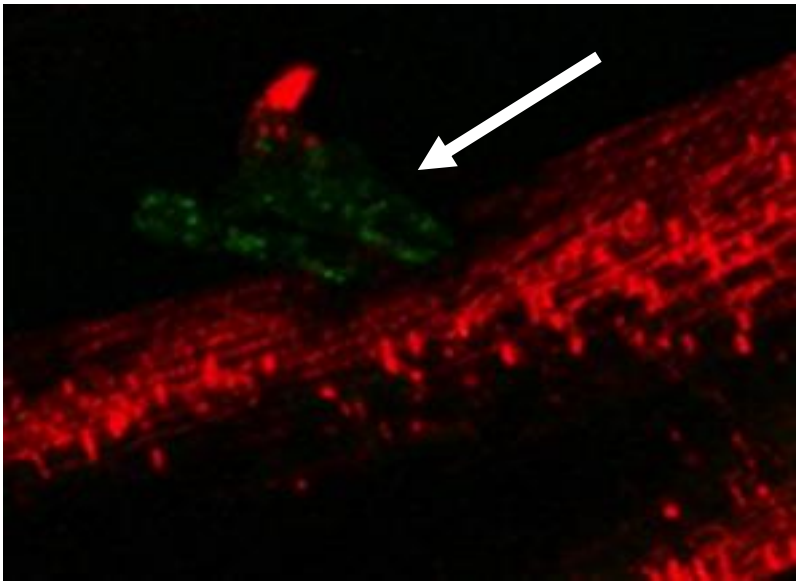

Figure 2: Early example of *Rotylenchulus reniformis*-cotton real-time interaction. An example of one of the first cotton-nematode real-time analysis images with arrow pointing to green (FITC) fluorescing reniform nematode.

1.10 MATERIAL AND METHODS

Rotylenchulus reniformis preparation.

Reniform nematodes were harvested from inoculated cotton grown in the Plant Science Research Center (PSRC) greenhouse located at Auburn University, AL. Initially, RN were collected as described below from the RN stock cultures maintained on cotton in the greenhouse. Cotton (Fibermax 1944 GLB2; Bayer CropScience, Research Triangle Park, NC) were grown in the 500 cm^3 pot for 60 days to increase egg levels. Soil used in the greenhouse was a Kalmia loamy sand (80 % sand, 10 % silt and 10 % clay) collected from the Plant Breeding Unit located at the E.V. Smith Research center of Auburn University, AL. Four cotton seeds were planted per pot and RN inoculated at the time of planting. Cotton plants were watered as needed to maintain soil moisture between 40 % and 60 % of the field capacity.

After 60 days, shoots were removed from the cotton plants and gently washed to remove soil. The RN eggs were extracted from the cotton roots following a modified version of the methodology of Jenkins (1964). The root mass was placed in 10% bleach (NaOCl) solution in a shaker for 5 minutes at 1 g-force on a Barnstead Lab Line Max Q 5000 E Class shaker (Conquer Scientific, San Diego, CA). Roots were then scrubbed by hand, eggs collected on a 25 µl pore sieve and washed into a 50 mL centrifuge tube. The contents were centrifuged at 427 g-forces for 1 minute in a 1.14 specific gravity sucrose solution (Viglierchio and Schmitt, 1983). Supernatant solution containing eggs were recollected on a 25 µm pore sieve, rinsed with water to remove sucrose from the eggs. Eggs were then placed in a mesh strainer in a bowl and placed on a heating pad (30°C) for 6-7 days, which allowed enough time for them to hatch.

Laser scanning confocal microscopy.

To further understand the nature of the reniform nematode autofluorescent material, visual observation using confocal microscopy was used to obtain z-series images of a clear J2 RN, different life stages of RN and two other plant parasitic nematodes, root-knot and soybean cyst nematodes.

The first step to using the confocal microscope (located in Rouse Life Science Building, Auburn University), was to turn the program on by pressing marked buttons 1-8 in order. Cotton roots were stained in 2', 7'-dichloroflurescin diacetate for about 30 min and transitioned to propidium iodide stain while confocal and computers started up. Once all the equipment is running, the NIS Elements program was opened and "Chap 4" button was pressed to start a new project. The "A1 Settings" windows were clicked, the scan mode "Resonant" was selected, the "Optical Path" window was opened and "Ch2" (green filter), "Ch4" (red filter) and "In" (light filter) Transmitted Detector checkboxes were selected. Cotton root was retrieved from PI stain, a desired secondary root removed with forceps and placed in a drop of deionized water on a glass slide with a coverslip on top. The slide was placed under microscope and "Eye port" button clicked on the program to visualize and adjust slide through the eye piece lens. Course and fine focus was adjusted and 10x magnification selected. Lights were shut off and "Scan" button clicked to examine slide. Z series image was captured by selecting "Acquire" tab, "Z-Series" tab to open the "Capture Z-Series" dialog box. Press the "Reset" button to start a new image. The mouse or the adjustment knob was scrolled to the top of the root on the screen and clicked on the "Top" button to select start point of Z-series. The selection point was scrolled down to desired bottom of the root and "Bottom" selected to choose end of the Z-series. The system automatically selected how many images within the Z-series it will take and can be changed (the larger number of images, the

higher the resolution the picture will be). The Dialog tab displayed how many µm the range of the Z-series is and how many µm between each picture is captured. We did not collect these data because over 100 Z-series images were taken over the course of the confocal studies. The “Run” button was pressed to start Z-series. The process takes an average of 3-5 minutes to complete depending on root thickness. Once completed, the file was saved to a folder on the computer to save the raw Z-series. The “Merge” button in the toolbar was selected to combine of the Z-series images into one. The LUT (Look up tables) tab was selected if pixel adjustment is needed. The “Scale” button located on the left vertical toolbar was selected to insert a scale on the image and adjusted to desired scale. Lastly, “ctrl” and “z” were selected together to bring image to new window and file was saved as an image file.

Fluorometric analysis.

Parameters of florescence, the intensity and wavelength distribution of emission spectrum, was determined through 300 to 700-nm after excitation at 425-nm, using the Cytation3 Image Reader ™ (BioTek Instruments, Winooski, VT). Once collected by the centrifugation at 6,000 rpm, juvenile 2 staged RN were homogenized using a small pestle and a mortar in 5 % (v/v) methanol and centrifuged at 10,000 rpm. Supernatant (referred as “total extracts”, hereafter) was then pipette-collected, and filtered twice through Whatman papers. The parts of total extracts were directly subjected to the fluorometer for the characterization of the chemical and physical nature of RN-derived autofluorescent substance and the rest were subjected to the high-performance liquid chromatography (HPLC) (Agilent 1260 Infinity Quaternary LC System equipped with a Diode Array Detector (DAD) VL+) in water to methanol method (5 % to 100 %) with a flow rate at 4.6 x 150 mm, 2.7 µm. The chromatogram was monitored and recorded by the absorbance

wavelength at 278 nm and the material associated with each peak was collected; approximately 100 to 200 µL of each fraction was subsequently subjected to the fluoremeter to determine and isolate RN-derived autofluorescent compound.

Florescence parameters of total extracts were measured every hour (e.g., 0 to 4 hr) while incubating with various concentrations of Dithiothreitol or hydrogen peroxide (e.g., 5, 10, 25, 50, and 100 µM), or a range of pH (e.g., 3.3, 4.8, 5.9, 7.0, 8.0, and 9.2). The pH solutions were made using Tris-HCl. The negative control was determined by averaging all measurements at 0 hr time.

Liquid chromatography/ mass spectrometry (LC/MS) & nuclear magnetic resonance (NMR).

HPLC fractions with the highest fluorescent signals were combined and concentrated using nitrogen gas and re-suspended with 0.05 % formic acid. Samples were given to collaborator Dr. Melissa Boersma, Chemistry Department, Auburn University, AL and subjected to the LC/MS (Waters Acquity UPLC and Q-Tof Premier) for small molecule analysis and structuring.

For further conformation, separate HPLC fractions with the highest fluorescent signal were combined and concentrated using nitrogen gas and re-suspended with deuterated chloroform, a commonly used solvent for NMR use. Samples were given to NMR director, Dr. Michael Meadows and both proton and carbon (C13) spectrums were analyzed to determine the molecular formula of the RN autofluorescent molecule.

1.11 RESULTS

Rotylenchulus reniformis autofluorescent metabolites in their intestinal tract

During experimentation on the visualization of the "real-time" interactions of live cotton roots and phytonematodes (e.g., RN) using a series of confocal and epi-fluorescent microscopies, we were able to repeatedly notice that RN accumulates autofluorescent substances. Initially, we speculated that those autofluorescent materials came from soils. However, we were able to confirm the accumulations of autofluorescent substances in RN using confocal microscopy, even after multiple and stringent washing steps (Fig. 3). In fact, the autofluoresent signal was clearly detectable as early as the egg stage of RN (Fig. 4), concurring with a conclusion that the RN-derived autofluorescent compound is an intrinsic substance of RN. Interestingly, the green signal resided primarily in the intestinal tract of RN, suggesting that this compound could play a critical role in cellular metabolisms and/or organismal physiology.

Rotylenchulus reniformis accumulate autofluorescence substance throughout lifespan

Previously, an autofluorescent compound found from *C. elegans*, namely lipofuscin, was reported as an age-related pigment (Pincus 2016). Therefore, we assessed if the production and accumulation of the RN-derived autofluorescent substance is also age and/or perhaps sex-dependent (Fig. 3). However, our confocal microscopy images displayed green fluorescence signal across egg to juvenile and mature stages, and in both male and female RN. These observations suggest that the autofluoresence compound plays a role in RN throughout their life-span.

Green autofluorescent compounds are intrinsic in other species of PPN including M. incognita and H. glycines.

To understand if RN is the only PPN that produces the autofluorescent substance, two other economically important PPNs were imaged using the confocal microscopy. As shown in Figure 5, both root-knot (*M. incognita)* and soybean cyst (*H. glycines)* nematodes are also able to emit autofluorescent signals. Furthermore, they accumulate autofluorescent substance, similar to RN, in their intestinal tracts. These results suggest that three PPN produce the same fluorescent or a similar compound, and utilize it in the same metabolic pathways, highlighting the critical roles and functions of this unknown metabolite in basic growth and survival of three, if not more, PPN.

Rotylenchulus reniformis-derived autofluorescence is stable across a broad range of pH and redox homeostasis.

As an initial step to understand the physical and chemical natures of RN-derived auto-fluorescent substance, we investigated its optimal range of excitation and emission wavelengths (Fig. 6). The HPLC-purified fraction with the highest excitation/emission lengths at 488/510-nm was scanned through a spectrum of excitation (488 nm) and emission (278) wavelengths. Interestingly, average values of the optimum excitation and emission of RN-derived fluorescence substance exhibited a unique spectrum of a maximum excitation of 425-nm and maximum emission spectrum of 525-nm with a relative intensity of 1400 W/m^2. We then examined physical stability of the RN-derived autofluorescent substance in several chemical conditions with excess to moderate levels of pH, H_2O_2 and DTT (see Materials and Methods, Fig. 7). Unexpectedly, based on the common nature of most fluorescent compounds, the RN-derived autofluorescent substance

are highly stable to, first of all, longer-term storage and light exposure, as well as changes in pH, H_2O_2 and DTT conditions (Fig. 7). There was a minor change in depreciation of fluorescence intensity of RN-derived autofluorescence throughout 3 to 4-week storage period at 4 ^oC in a micro-centrifuge tube. Furthermore, over the 4-hr period, RN-derived autofluorescence incubated in pH 3.3 and pH 8.0 showed decreases in intensity of only approximately 30 W/m^2 (Figure 7A). Note that RN-derived autofluorescence was more stable in excess basic than acidic pH that it decreased a fluorescent intensity only about 10 to 20 W/m^2 in pH 9.2, whereas showing the intensity decreases of about 100 to 175 W/m^2 at pH 4.8, 5.9 and 7.0 (although it is less than 25 % of original intensity). Similarly, treatment of DTT and H_2O_2 reduced the intensity of RN-derived autofluorescence, over a 4-hr period, approximately 195 (< 50 %) and 130 (< 25 %) W/m^2, respectively (Fig. 7B and C). Overall, the RN-derived autofluorescence quenched slightly when treated with a range of concentrations of pH, H_2O_2 and DTT over the course of 4-hr. However, in consideration of nature of other fluorescence, RN-derived autofluorescence did not decimate completely, and likely considered as highly stable.

Rotylenchules reniformis-derived autofluorescent compound identification.

To identify and determine chemical identity of RN-derived autoflurescence, we first subjected the sample to HPLC to fraction out the most autofluorescent portions. Then the most autofluorescent fractions were combined and subjected to MS and then MS/MS to use electric and magnetic fields to measure the weight of the sample's charged particles. Lastly, the sample was subjected to NMR to determine the content and purity of the sample to further determine molecular structure. Our collaborators, Dr. Victoria Owens and MS lab director Dr. Melissa Boersma, narrowed down formula candidates by analyzing the most prominent peaks that are both in spectra

and performed a search of possible molecular formulas that match the weight. Next, the formulas were compared and narrowed down by overlapping them to the list. NMR data showed the 8.5 ppm peak is indicative of a Sulfonium, [(17β) -3-ethoxyestra-1, 3,5(10)-trien-17-yl]ethylmethyl-(9CI). This structure includes one sulfonium, one benzine ring, three cyclohexanes, four hydrogens, and an ethyl methyl group.

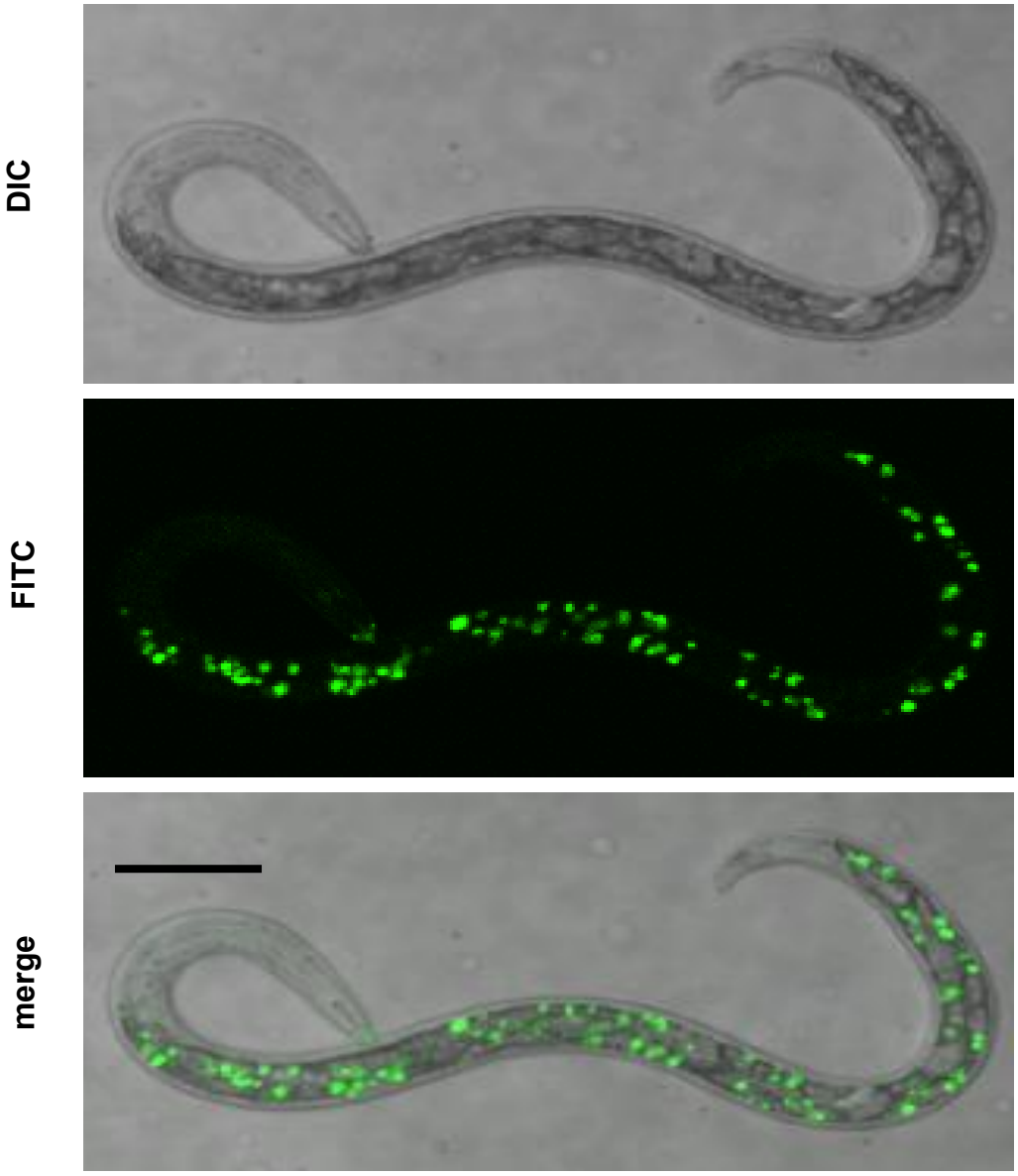

Figure 3: *Rotylenchulus reniformis* autofluorescence resides in intestinal tract. Laser scanning confocal microscopy imaging unveils natural autofluorescence signals in the intestine areas of RN. DIC: bright field image. FTIC: green fluorescein image with the emission wavelength at 505 to 570-nm bandpass. Measurement line is 60 µm.

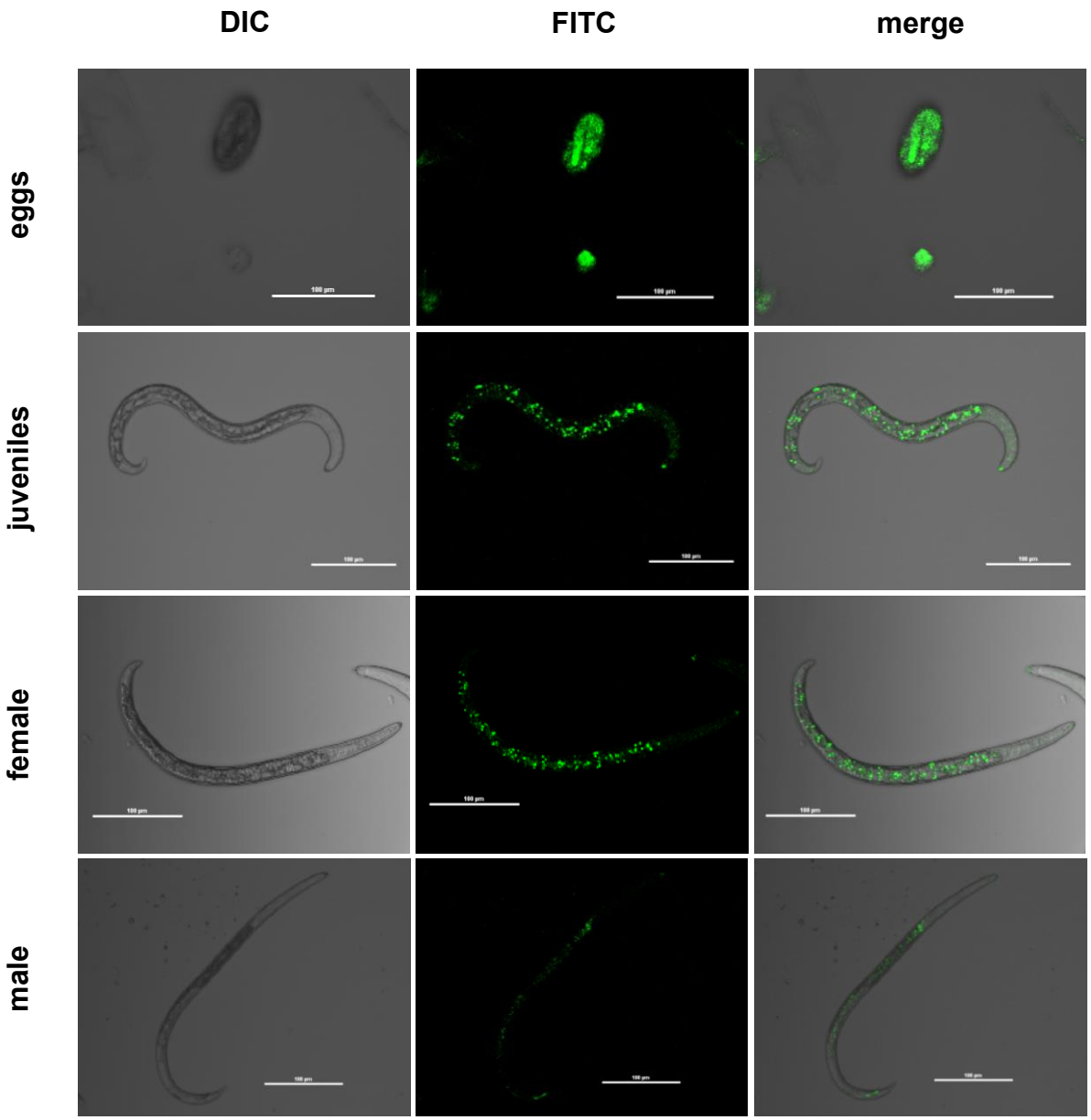

Figure 4: *Rotylenchulus reniformis* accumulate the autofluorescent compound throughout their life cycle. Laser scanning confocal microscopy visualizes green autofluorescent signals at 488-nm excitation from all growth stages including the egg, juvenile and mature stages of both female and male RN. DIC: bright field image. FTIC: green fluorescein image with the emission wavelength at 505 to 570-nm bandpass. Measurement line is 100 µm.

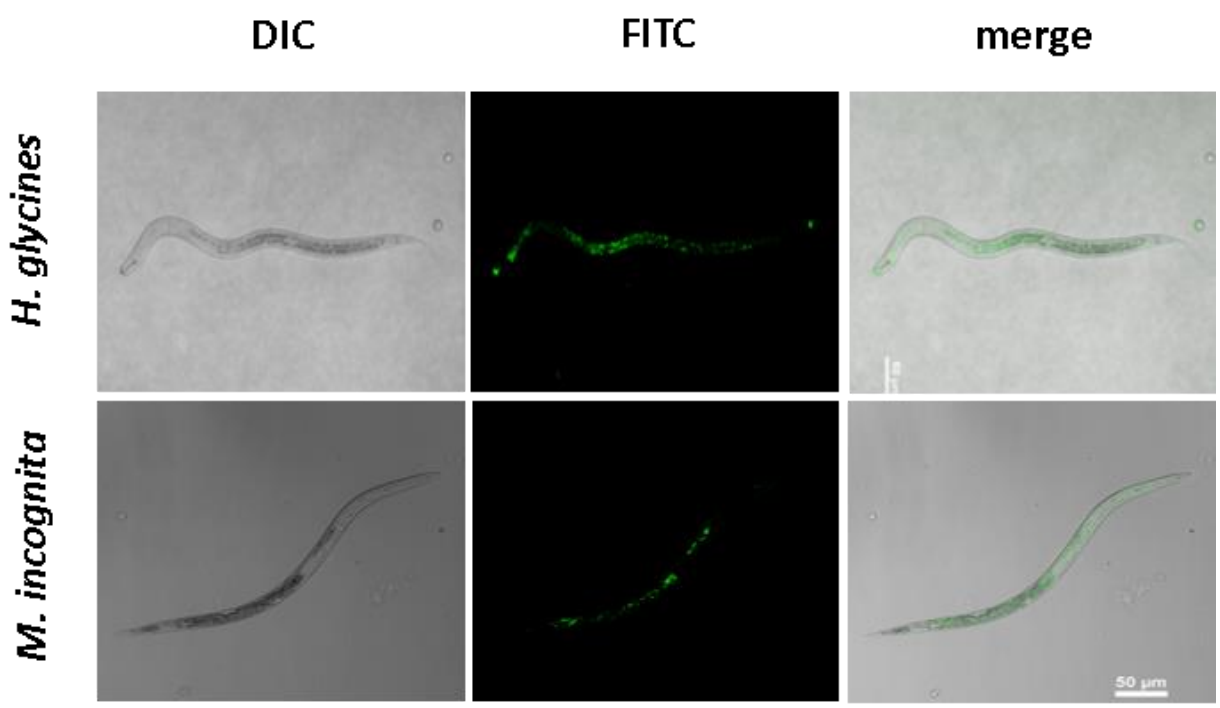

Figure 5: *Heterotera glycines* and *Meloidogyne incognita* are also able to accumulate natural autofluorescent substance in their intestinal tract. *H. glycines* and *M. incognita* were subjected to laser scanning confocal microscopy imaging. DIC: bright field image. FTIC: green fluorescein image with the emission wavelength at 505 to 570-nm bandpass. Measurement line is 50 µm.

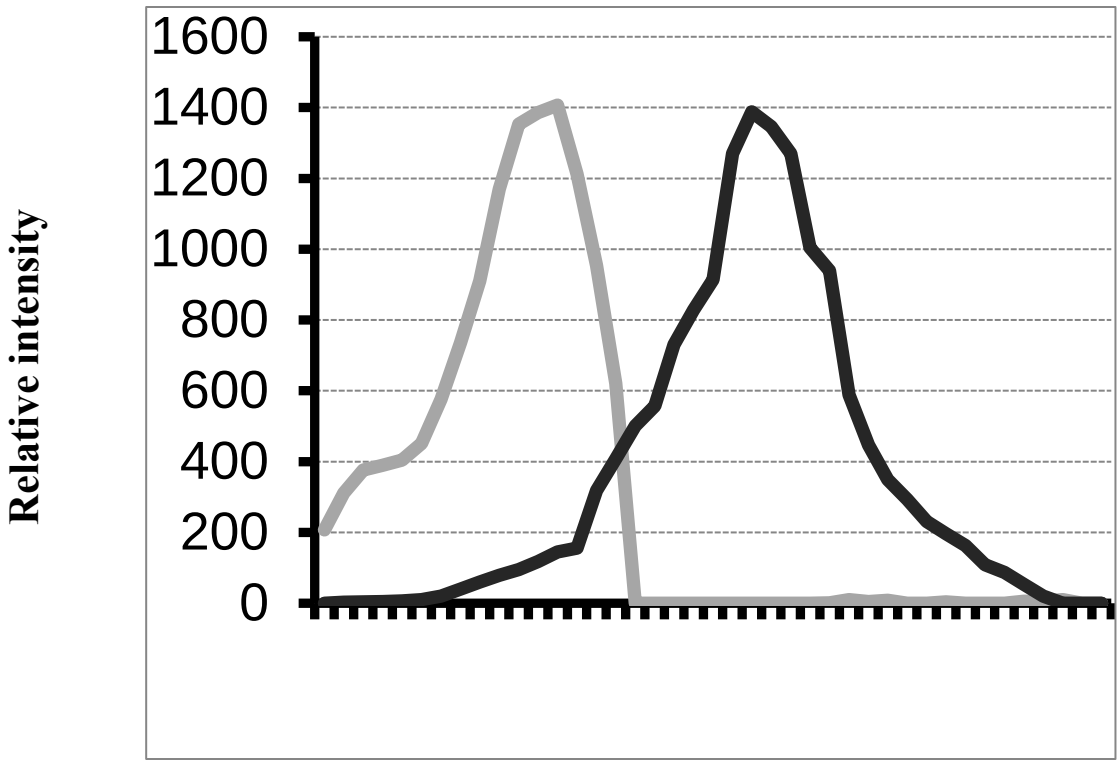

Figure 6: *Rotylenchulus reniformis*-derived autofluorescence exhibits a unique excitation and emission spectrum. A unique spectrum of RN-derived autofluorescence exhibits a maximum excitation (black line) collected at 425-nm, and maximum emission (grey line) spectrum collected at 525-nm with a relative intensity of 1400 W/m^2 by a multi-mode fluorometer (Cyatation3^{TM}).

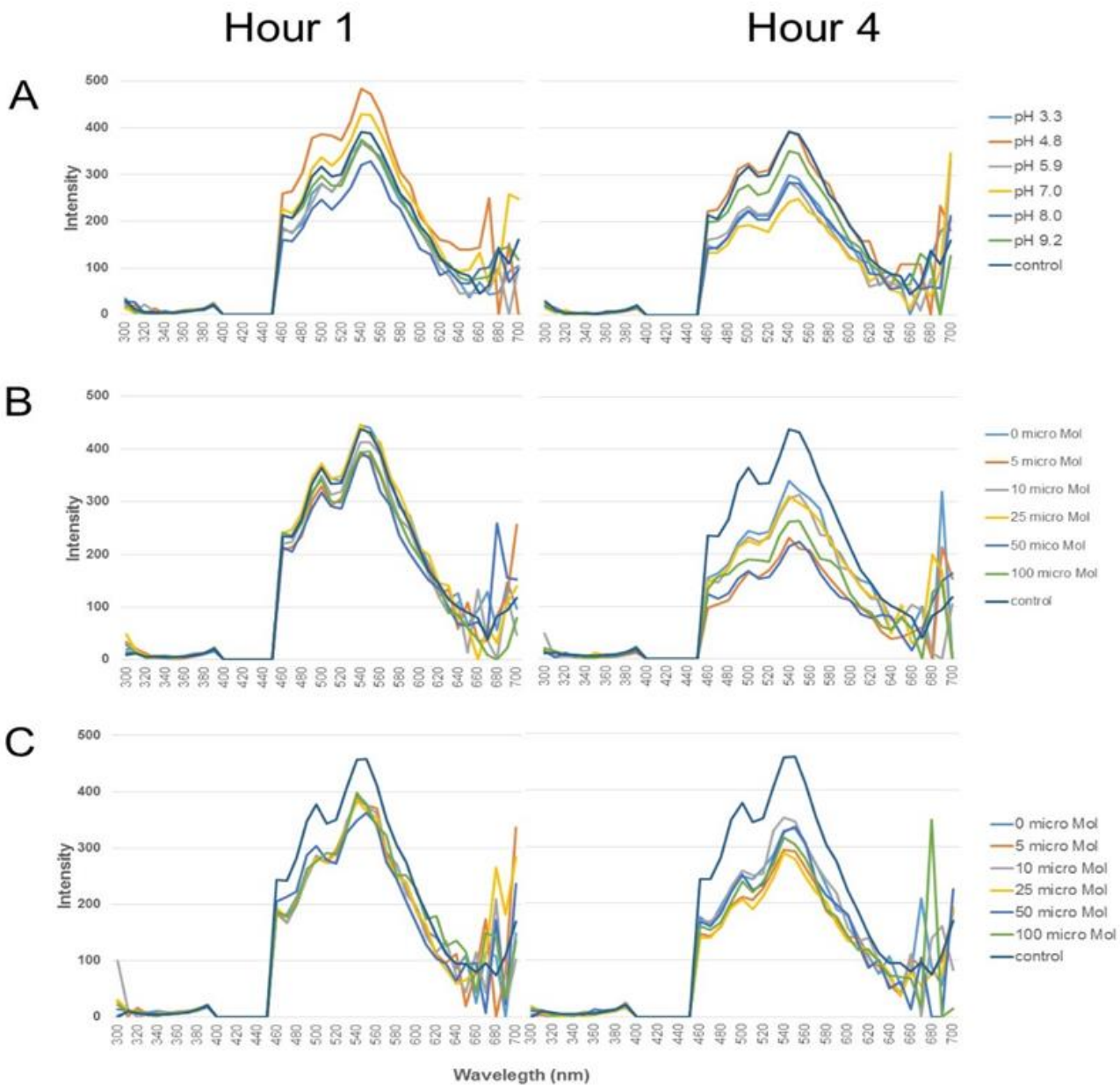

Figure 7: Average intensity of *Rotylenchulus reniformis*-derived autofluorescence under different pH and redox homeostatic conditions. Average readings of the relative fluorescence intensity of RN-derived autofluorescence during incubating at various pH levels ranged from 3.3 to 9.2 (**A**), DTT concentrations from 0 to100 µM (**B**), and H_2O_2 concentrations from 0 to100 µM (**C**).

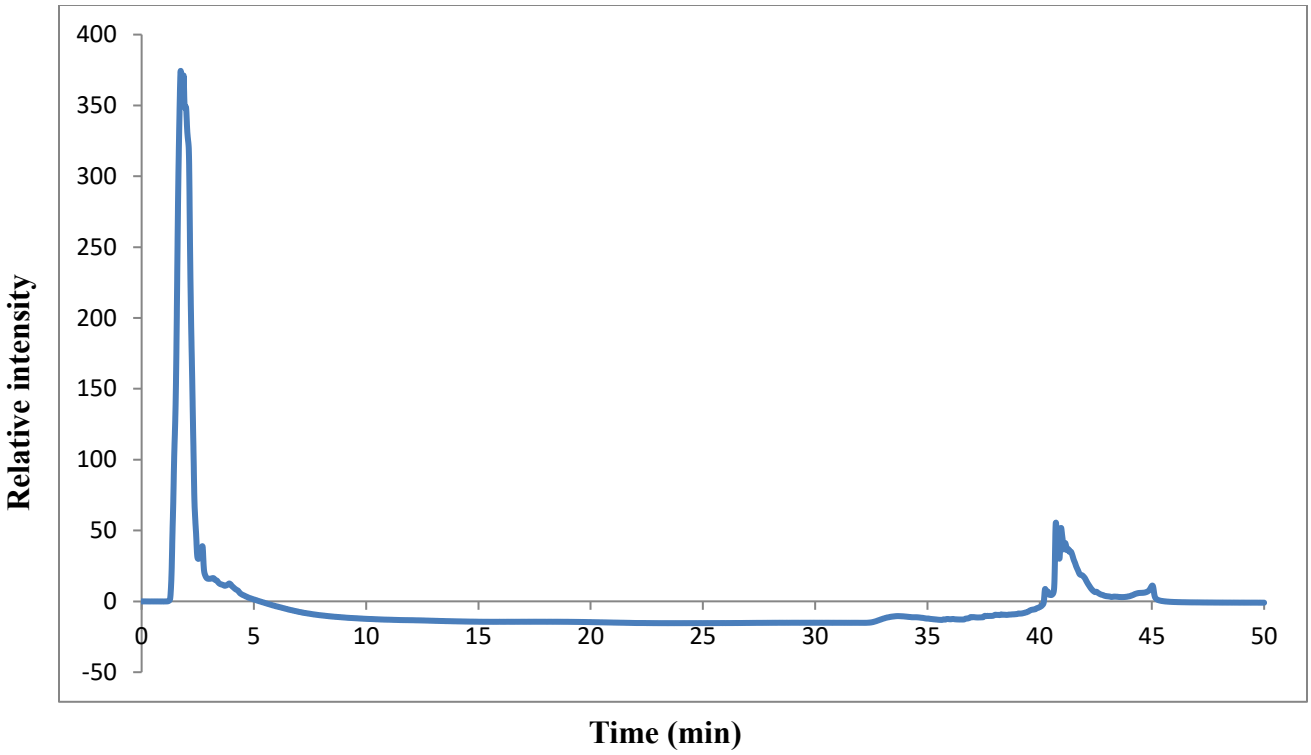

Figure 8: High performance liquid chromatography data. Injection of the RN-derived autofluorescent solution was subjected directly into the C18 column and using a water to methanol (polar to non-polar) phase change (5%-100%). The peak of the compound was found between 40-45 minutes.

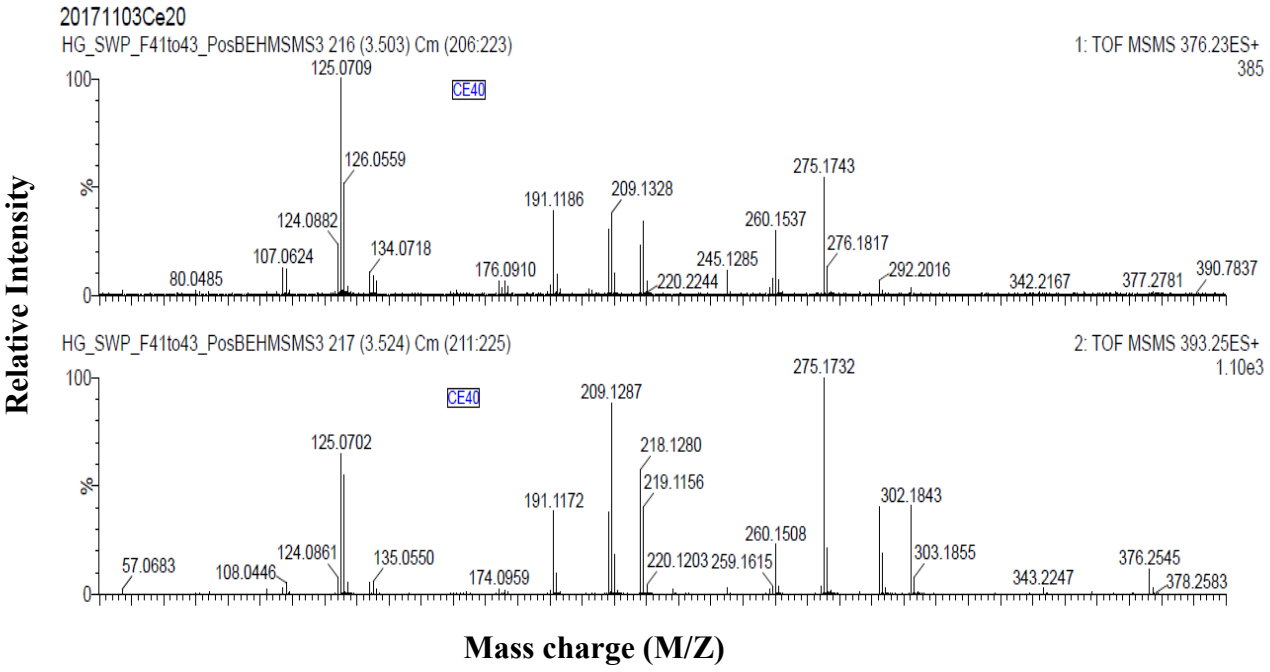

Figure 9: MS/MS spectra. The MS/MS RN-derived autofluorescent molecule data shows mass-to-charge ratios to assist in determining identity of the structure.

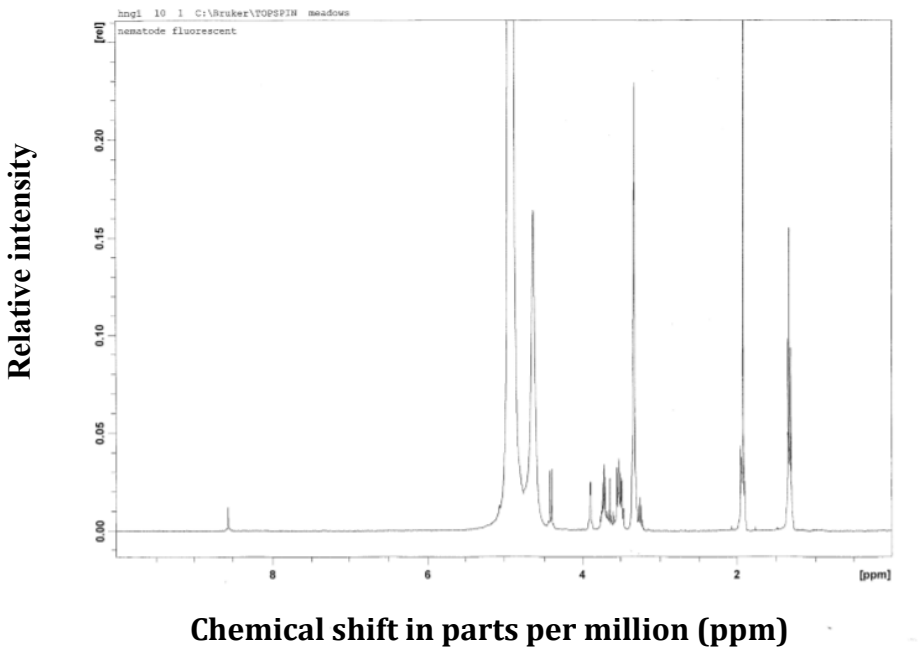

Figure 10: NMR proton spectra. The nuclear magnetic resonance of the RN-derived autofluorescent molecule has major peaks between 1-6 ppm.

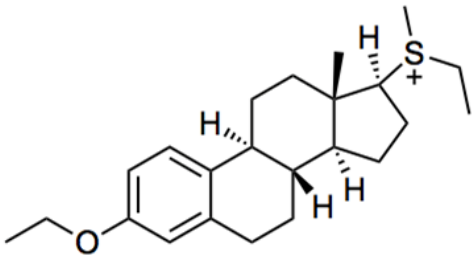

Figure 11: Structure of Sulfonium, [(17β) -3-ethoxyestra-1,3,5(10)-trien-17-yl]ethylmethyl- (9CI). The RN-derived autofluorescent structure includes one sulfonium, one benzine ring, three cyclohexanes, four hydrogens, and an ethyl methyl group.

1.12 DISCUSSION

Reniform nematode, among other phytonematodes has been observed to autofluoresce naturally. Autofluorescence is the natural emission of light by biological structures such as mitochondria and lysosomes when they have absorbed light and is used to distinguish the light originating from artificially added fluorescent markers (fluorophores) (Monici 2005). Many bacteria, actinomycetes, algae, and fungi fluoresce naturally in ultraviolet light; and the presence of invading organisms, especially actinomycetes, has been detected clinically, as well as in plants and animals, by this method (e.g. invasion of potato by *Streptomyces scabies* (Darken 1960). The most common autofluorescent molecules are NADPH and flavins; the extracelluar matrix can also contribute to autofluorescence for their intrinsic properties such as collagen and elastin (Monici 2005). Generally, proteins containing an increased amount of the amino acids tryptophan, tyrosine and phenylalanine show some degree of autofluorescence (Menter 2006). Autofluorescence occurs in non-biological materials found in textiles. Autofluorescence from U.S. paper money has been demonstrated as a means for discerning counterfeit currency from authentic currency (Chia 2009). Autofluorescence is useful and can illuminate the structures of interest or serve as diagnostic indicators (Monici 2005). For example, cellular autofluorescence can be used as an indicator of cytotoxicity without the need to add fluorescent markers (Fritzsche 2010). Known molecules that autofluoresce in animals include NAD(P)H, collagen (Georgakoudi *et al.* 2002), retinol, riboflavin, cholecalciferol, folic acid, pyridoxine (Zipfel *et al.* 2003), tyrosine, dityrosine (Menter 2006), indolamine, lipofuscin (Schönenbrücher *et al*. 2008)., tryptophan, flavin and melanin (Gallas 1987).

Autofluorescent material was first described in *C. elegans* 175 years ago (Hannover 1842). Autofluorescence is generally described as an “age pigment” or lipofuscin and when viewed *in*

vivo, it fluoresces in yellow to red wavelengths when excited with UV or blue light (Yin 1991). It consists of highly-oxidized, insoluble cross-linked proteins and lipids, yet exact special properties and precise chemical nature or the material varies across tissues and organisms (Yin 1996). In *C. elegans*, autofluorescence has long been noted to correlate with aging and, as in mammalian cells, much of it is confined to intracellular granules of lysosomal origin, specifically within the intestinal cells for *C. elegans* (Clokey 1986).

In studies focusing on aging and health of individuals, the use of accumulation of intestinal autofluorescence in *C. elegans* is measured. Moreover, there is little standardization regarding excitation/emission wavelengths to use for this analysis. Different studies focus on different colored autofluorescence but typically focus on UV excitation with blue emissions or green-to-red color (Davis 1982). Recent work using data from both *in vivo* and in solvent extracts has shown that several hours before and after death, individuals become more autofluorescent (Coburn 2013).

Overall, RN autofluorescence proves to be a useful characteristic for identification of RN in plant-nematode interaction studies using confocal microscopy. The green autofluorescence against the red PI stained root membranes creates high-resolution images for detection of RN infecting root hosts. The autofluorescence is also an indicator of viability and life (Forge and MacGuidwin, 1989). RN autofluorescence occurs throughout the life cycle, from egg, juvenile and through adulthood. The RN autofluorescence is unique because of its maximum excitation spectrum collected at 425 nm. This excitation is different from that of *C. elegans*, which has a maximum excitation of 470 nm (Pincus 2016). However, the maximum emission of both RN and *C. elegans* is 525 nm. In addition to green autofluorescence, *C. elegans* exhibits red and blue fluorescence, relating to senescence (Pincus 2016), whereas RN does not.

The RN autofluorescent material is a stable compound with little degradation over time. Treatment with DTT, a reducing agent, is frequently used to reduce the disulfide bonds of proteins by decreasing the number of binding sites or to prevent intramolecular and intermolecular disulfide bonds from forming between cysteine residues of proteins (Vauquelin 1979). The different concentrations of DTT decreased the fluorescence intensities more disjointedly than those of the H_2O_2 levels, which decreased contiguously. However, the compound still had fluorescent qualities under these conditions, showing its stability. The fluorescent material had a higher intensity at acidic levels of pH, which is understandable because the autofluorescent material is found in the acidic intestinal tract, where breakdown of nutrients occurs (Smith 2003).

Autofluorescence was observed to reside not just in RN, but the other economically important phytonematodes, root-knot (*Meloidogyne incognita)* and soybean cyst (*Heterodera glycines*. Future aims could focus on differences or similarities, if there are any, between RN, root-knot and soybean cyst nematodes.

In conclusion, the fluorescent compound was found to be stable throughout the RN life cycle, occur in other species of phytonematodes, and be structured as Sulfonium, [(17β) -3-ethoxyestra-1, 3, 5(10) -trien-17-yl] ethylmethyl-(9CI). RN autofluorescence is important mainly because it aided in RN-cotton interaction research, visualizing where the RN are when infecting cotton. However, this compound has the potential to be processed and used for research purposes in the future.

1.13 LITERATURE CITED

Berger, S., A. K. Sinha, T. Roitsch. 2007. Plant physiology meets phytopathology: plant primary metabolism and plant-pathogen interactions. 58 (15-16): 4019-4026.

Chalfie, M. 1995. Green fluorescent protein. Photochemistry and photobiology 62: 4.

Chia, T. and M. Leven. 2009. Detection of counterfeit U.S. paper money using intrinsic fluorescence lifetime. Optics Express 17 (24): 22054-22061.

Clokey, G.V., L. A. Jacobson. 1986. The autofluorescent "lipofuscin granules" in the intestinal cells of *C. elegans* are secondary lysosomes. Mech Ageing Dev 35(1):79-94.

Coburn, C., *et al*. 2013. Anthranilate fluorescence marks a calcium-propagated necrotic wave that promotes organismal death in *C. elegans*. PLoS Biol. 11(7): e1001613.

Darken, M. A. 1960. Microbiological process report: natural and induced fluorescence in microscopic organisms. Biochemical Research Station, American Cyanamid Company, Pearl River, New York. 354-360.

Davis, B.O. Jr, G. L. Anderson, D. B. Dusenbery. 1982. Total luminescence spectroscopy of fluorescence changes during again in C. elegans. Biochemistry 21(17):4089-95.

Forge, T. A. and MacGuidwin, A. E. 1989. Nematode autofluorescence and its use as an indicator of viability. Journal of Nematology 21(3):399-403.

Fritzsche, M. and C. F. Mandenius. 2010. "Fluorescent cell-based sensing approaches for toxicity testing". Anal Bioanal Chem. 398 (1): 181–91. doi:10.1007/s00216-010-3651-6. PMID 20354845.

Gallas, J. M. and M. Eisner.1987. "Fluorescence of Melanin-Dependence upon Excitation Wavelength and Concentration". Photochem. Photobiol. 45 (5): 595–600.

Gazaway, W. A., K. S. Lawrence, C. D. Monks, J. R. Akridge. 2007. Crop rotation- an effective tool for managing reniform nematodes in cotton. Auburn University, 104 Extension Hall, Auburn University, AL 36849.

Georgakoudi, I. *et al*. 2002. NAD(P)H and collagen as in vivo quantitative fluorescent biomarkers of epithelial precancerous changes. Cancer Res. 62 (3): 682–687.

Hannover, A. 1842. Mikroskopishe Undersogelser af Nevensystem. Natrurv. Math. Ajh. Copenhagen 10:1–112.

Hedgecock, E. M., J. G. Culotti, J. N. Thompson, L. A. Perkins. 1985. Axonal guidance mutants of *Caenorhabditis elegans* identified by filling sensory neurons with fluorescin dyes. Developmental Biology 111:158-170.

Jenkins, W.R. 1964. A rapid centrifugal-flotation technique for separating nematodes from soil. Plant Disease Report. 48:692.

Koenning, S. R., T. L. Kirkpatrick., J. L. Starr, J. A. Wrather, N. R. Walker, J. D. Mueller. 2004. Plant-parasitic nematodes attacking cotton in the United States: old and emerging production challenges. The American Phytopathological Society. Plant Disease 88 (2): 100-113.

Menter, J. M. 2006. Temperature dependence of collagen fluorescence. Photochem Photociol, Science. 5 (4): 403-410.

Monici, M. 2005. "Cell and tissue autofluorescence research and diagnostic applications". Biotechnol Annu. Rev. 11: 227–56. doi:10.1016/S1387-2656(05)11007-2. PMID 16216779.

Nicol, J. M. et al. 2011. Current nematode threats to world agriculture. Genomics and Molecular Genetics of Plant-Nematode Interactions: 21-43.

Pincus, Z., T. C. Mazer, F. J. Slack. 2016. Autofluorescence as a measure of senescence in *C elegans*: look to red, not blue or green. Aging 8(5):889-98.

Schönenbrücher, H. *et al*. 2008. "Fluorescence-Based Method, Exploiting Lipofuscin, for Real-Time Detection of Central Nervous System Tissues on Bovine Carcasses". Journal of Agricultural and Food Chemistry. 56 (15): 6220–6226.

Shakir, M. A., J. Miwa, S. S. Siddiqui. 1993. A role of ADF chemosensory neurons in dauer formation behaviour in *Caenorhabditis elegans*. Neuroreport 4:1151-1154.

Shroeder, N. E. and A. E. MacGuidwin. 2007. Incorporation of a fluorescent compound by live *Heterodera glycines*. Journal of Nematology 39(1):43-49.

Smith, J. L. 2003. The role of gastric acid in preventing foodborne disease and how bacteria overcome acid conditions. Journal of Food Protection: 66 (7): 1292-1303.

Turman, A. and Brunk, U. T. 2006. Oxidative stress, accumulation of biological 'garbage', and aging. Atioxid Redox Signal. 8:197-204.

Vauquelin, G., S. Bottari, L. Kanarek, A. D. Strosberg. 1979. Evidence for essential disulfide bonds in adrenergic receptors of turkey erythrocyte membranes. The Journal of Biological Chemistry 254: 4462-4469.

Viglierchio, D. R., R. V. Schmitt. 1983. On the Methodology of Nematode Extraction from Field Samples: Baermann Funnel Modifications. Journal of Nematology 15(3):438-444.

Yin, D. Z., U. T. Brunk. 1991. Microfluorometric and fluorometric lipofuscin spectral discrepancies: a concentration-dependent metachromatic effect. Mech Ageing Dev. 59(1-2):95-109.

Yin, D Z.1996. Biochemical basis of lipofuscin, ceroid, and age pigment-like flurophores. Free Radic Biol Med. 21(6):871-88.

Zipfel, W. R., R. M. Williams, R.Christie, A. Y. Nikitin, B. T. Hyman, W. W. Webb. 2003. Live tissue intrinsic emission microscopy using multiphoton-excited native fluorescence and second harmonic generation. Proceedings of the National Academy of Sciences of the United States of America. 100 (12): 7075–7080.

CHAPTER 3: PLANT DEFENSE ACTIVITY OF GOSSYPIUM STRAINS AGAINST ROTYLENCHULUS RENIFORMIS

1.14 ABSTRACT

Plant parasitic nematodes (PPN) are major cotton pathogens and of considerable economic importance worldwide, causing an ever-increasing yield loss of an estimated 10 % annually. Lately, reniform nematode (RN, *Rotylenchulus reniformis*) has become a major threat to the cotton farming industry across the southeastern U.S. However, current pest management programs lack **a)** resistant cultivars, **b)** efficacious crop rotation and **c)** effective and low cost nematicide and is in urgent need of a breakthrough but it is not necessarily forthcoming due to a narrow genetic diversity in the cotton cultivars and germplasms, as well as little knowledge on the defense physiology of cotton-phytonematode interactions.

Hypersensitive response (HR) is the most eminent and effective innate defense system in plants, whereby host resistance (*R*)-genes recognize effector proteins derived from pathogens and develop programmed cell death (PCD) within a small perimeter of infection sites, thus preventing the spread within the plant and multiplication of pathogens. Indeed, it has long been proposed that plant roots could develop HR upon and limiting the establishment and spread of PPN (Rice et al. 1985, Anthony *et al.* 2005, Agudelo *et al*. 2005, Mur, 2008, Sikkens 2011, Khallouk *et al*. 2011, Cabasan *et al.* 2014), but this hypothesis has not properly been validated. Hence, this study has employed a laser scanning confocal microscopy system to monitor the real-time interactions of 'live' PPN (e.g., RN) with cotton roots. As reported, PPN infections led to the rapid bursts of reactive oxygen species (ROS such as H_2O_2), one of the early plant responses upon various environmental stresses. However, cotton roots did not activate PCD, and not even localized cell

death (LCD, physical injury), suggesting that RN-led damages are limited to those cells where RN physically invaded. On the other hand, we observed that the tolerance levels of cotton roots against PPN are highly correlated with the amount of root hairs produced in the lateral root systems, indicating the possible importance of root growth and morphology in plant and PPN interactions. Now, to further scrutinize our hypothesis, we are employing a systematic biology approach to discern **i**) the tolerance associated genes and **ii**) if those genes are involved in root organogenesis by analyzing differential transcriptomes between the tolerant and susceptible cotton germplasms before and after nematode infections.

1.15 INTRODUCTION

Cotton, *Gossypium* spp., is the most important fiber crop, and grown in all tropical and subtropical countries. The U.S. is the world's third largest cotton producer which accounts for >$ 21 billion in products and services annually, generating more than 125,000 jobs in the industry sector from farm to textile mill (USDA ERS 2018). However, there are large arrays of damages and diseases that inflict cotton plants, causing significant yield losses. In 2017, various pathogens and herbivores caused ~10% losses in the yields of cotton crops worldwide; plant parasitic nematodes (PPN) caused the largest percent loss in the U.S., estimated at 4.65% (NCCA 2018). The yield losses caused by PPN have been steadily upward as from about 2% in the mid-1980s to the current levels (Weaver 2015). This increase is primarily due to a general lack of effective management tools, as well as of our understanding on the sensory modes and genetic resistance of host plants towards phytonematodes (Starr et al. 2007, Li et al. 2015).

A current model elucidating plant interactions and defense responses to PPN has been built on the basis of the hypothesis that plant roots operate essentially similar - if not the same - defense

machineries against phytonematodes as plant leaves do against other microbial pathogens and herbivores. This has been proposed since an earlier study (Bailey 1941) that isolated a single, dominant resistant (*R*)-gene (*Mi-1*) from a relative of tomato, *Lycopersicon peruvianum*, which confers resistance against some of root-knot nematodes (RKN, *Meloidogyne* spp.). *Mi-1* belongs to a nucleotide binding domain [NBD] and leucine-rich repeat [LRR] superfamily of which LRR regions demonstrated a hypersensitive response (HR)-like localized cell death on *Nicotiana benthamiana* leaves after transient expression (Hwang et al. 2000). Thus, large efforts have directed to espy phytonematode-derived effectors and avirulence (*Avr*)-genes that bind and trigger *R*-gene (e.g., *Mi-1*)-mediated resistance (also called, effector-triggered immunity [ETI]). In the last few decades, various transcription analyses of phytonematode secretory cells (i.e., esophageal gland cells) have successfully revealed several peptides and proteins (referred to as effectors) released from PPN stylets into the cytoplasm or apoplast of plant cells (reviewed in Mitchum et al. 2013, Hewezi and Baum 2013, Fosu-Nyarko and Jones 2016, Gillet et al. 2017). However, further investigation is needed to understand the role and function of those effectors in the ETI and immunophenotypes of host plants.

Thus far, two RKN effectors MAP-1 from *M. incognita* and Cg1 from *M. javanica* were proposed as cognate *Avr*-factors to Mi-1 (Glesson et al. 2008, Castagnone-Sereno et al. 2009), as both effectors were identified from avirulent strains displaying incompatible interactions with resistance plants carrying the *Mi-1 R*-gene (Semblat et al. 2001, Lozano-Torres et al. 2012). However, their direct or indirect interaction with Mi-1, and roles in triggering Mi-1-mediated resistance require further studies. On the other hand, effectors RBP-1 and VAP1 from potato cyst nematodes (PCN, *Globodera* spp.) demonstrated binding affinity to a canonical NLR or guardee protein such as a potato Gpa2 and a tomato $Rcr3^{pim}$/Cf-2, as well as the activation of defense

responses including a foliar HR upon transient expression (Sacco et al. 2009, Lozano-Torres et al. 2012). In addition, histological images of tomato roots carrying *Rcr3*^{pim}/*Cf-2* genes exhibited to a large extent a localized cell death response near the infection sites of PCN (Lozano-Torres et al. 2012), agreeing with a hypothesis that stereotypical ETI and HR play critical roles in the disease resistance of root tissues against phytonematode infections.

It has long been proposed that HR occurs in cells located near invading PPN (Rice et al. 1985). Microscopic imaging observed a layer of necrotic cells at the periphery of syncytium produced upon PCN infections, and those cell deaths were greater in number in resistant vs. susceptible potato lines although the reactions were comparatively slower than the typical HR. Since then, several studies have monitored similar, if not the same, HR-like responses in various plant cells towards PPN infections (Anthony et al. 2005, Agudelo et al. 2005, Khallouk et al. 2011, Cabasan et al. 2014) in parallel with accumulation of ROS and phenolic compounds, which are classic chemical signals of HR (Waetzig et al. 1999, Pegard et al. 2004, Melillo et al. 2006, 2011, Simmonetti et al. 2009). However, it is still unclear whether this HR-like phenomenon observed during PPN infections is a) an example of PCD or cell lysis, or b) correlated with root resistance towards PPN (Williamson and Kumar 2006). Thus is of particular interest considering that i) ROS productions are not the prerequisite of HR, instead could suppress cell death responses while promoting PPN infections (Siddique et al. 2014), as well as most if not all histological analyses conducted thus far ii) employed extensive fixation processes which potentially cause the physical and/or physiological alteration of cells (Santana et al. 2015), and iii) monitored HR-like responses at >3 d post PPN inoculations. The later, rather slower than the typical foliar HR (Rice et al. 1985, Mur et al. 2008), implies that PPN-induced root HR may be physiologically and biochemically

unique, or perhaps less effective. Alternatively, those cell deaths seen along with PPN infections are not PCD but physical damages (LCD).

Indeed, a previous study observed that HR-like responses in the roots of Lonren-1, once developed as resistance germplasm, concurs with progressive decreases in root mass upon increasing inoculums of RN defined in Chapter 1, which account for >60 % of cotton lost to all PPN (Sikkens et al. 2011, Doshi et al. 2010). Note that the HR-like trait of Lonren is deductively inherited from a parent line *Gossypium longicalyx*, an only known primitive accession of upland cotton (*G. hirsutum*) conferring strong resistance against RN (Agudelo et al. 2005, Robinson et al. 2007). This result indicates that the root HR-like responses may be impotent to limit PPN infections, but steadily extend necrosis across root tissues and lead to restricted root growth, re-inquiring if the RN (or PPN)-induced HR-like reactions are the 'true' PCD.

Therefore, the present study has employed a confocal microscopy to monitor the real-time interactions of 'live' RN with three cotton germplasms including LONREN-1 (hypersensitive), BARBREN-713 (tolerance) and SG-714 (susceptible). To determine the activation of PCD at the sites of PPN infections, target specific fluorophores such as propidium iodide and 2'7'-dichlorofluorescin were applied to cotton roots, and visualized cellular mortality and ROS productions during time-course imaging. Concurrently, we also have employed a systematic biology approach to isolate tolerance genes by analyzing differential transcriptomes between tolerant and susceptible/hypersensitive germplasms before and after nematode infections. In the end, our studies will provide genetic and molecular principles in tolerance and/or resistance mechanisms of plant roots against PPN, which will aid in engineering of defense responses, upgrading a plant's own survival and growth capacity, and improving yield for crop productions.

1. 15 MATERIALS AND METHODS

Rotylenchulus reniformis preparation

Reniform nematodes were harvested from inoculated cotton grown in the Plant Science Research Center (PSRC) greenhouse located at Auburn University, AL. Initially, RN were collected as described below from the RN stock cultures maintained on cotton in the greenhouse. Cotton plants (Fibermax 1944 GLB2; Bayer CropScience, Research Triangle Park, NC) were grown in the 500 cm^3 pot for 60 days to increase RN egg levels. Soil used in the greenhouse was a Kalmia loamy sand (80 % sand, 10 % silt and 10 % clay) collected from the Plant Breeding Unit located at the E.V. Smith Research Center of Auburn University. Four cotton seeds were sown per pot and RN inoculated at the time of sowing. Cotton plants were watered as needed to maintain soil moisture between 40 % and 60 % of the field capacity.

After 60 days, shoots were removed from the cotton plants and the roots were gently washed to remove soil. The RN eggs were extracted from the cotton roots following a modified version of the methodology of Jenkins (1964). The root mass was placed in 10% bleach (NaOCl) solution in a shaker for 5 minutes at 1 g-force on a Barnstead Lab Line Max Q 5000 E Class shaker (Conquer Scientific, San Diego, CA). Roots were then scrubbed by hand, eggs collected on a 25 µl pore sieve and washed into a 50 mL centrifuge tube. The contents were centrifuged at 427 g-forces for 1 minute in a 1.14 specific gravity sucrose solution (Viglierchio and Schmitt, 1983). Supernatant solution containing eggs was recollected on a 25 µm pore sieve, rinsed with water to remove sucrose from eggs. Eggs were then placed in a mesh strainer in a bowl and placed on a heating pad (30°C) for 6-7 days, enough time for them to hatch.

Plant growth condition and R. reniformis inoculation

Seeds of three cotton germplasms, Barbren, Lonren-1 and SG-747 (U.S. Department of Agriculture, Insect Control and Cotton Disease Research Unit, College Station, TX) were sterilized by immersing in 10 % (v/v) commercial Clorox (NaOCl) for 15 min, washed twice with 70 % (v/v) ethanol for 5 min, and rinsed twice with deionized H_2O. The seeds were then placed in damp germination paper, rolled up and placed inside a plastic bag, and incubated on a heat plate at 30°C to germinate for 3-4 days.

Once cotton seeds were germinated, the seedlings were carefully transferred to the 50 mL tubes filled to the brim with sandy-soil (Plant Science Research Center (PSRC), AU). Presence of RN was confirmed via Nikon TSX 100 inverted microscope at 20x magnification. Roughly, 2,000/ mL RN were inoculated via pipette to each of the cotton tubes. The cotton infected seeds were kept in a 12-hour light/dark growth chamber for two weeks and watered daily to keep soil moist.

Real-time analysis via confocal microscopy

Control (healthy) or RN-inoculated cotton roots were gently removed from the tubes, and carefully washed in water until most of the soil was removed from roots. The roots were then submerged in 2', 7'-dichloroflurescin diacetate (10 μM, ROS staining) for 30 min, rinsed with deionized H_2O. Subsequently, the roots were submerged in propidium iodide (PI, cellular membrane staining, 10 μg/mL) for 10 min and washed with deionized H_2O. Secondary roots were detached from the primary root using sterilized forceps and placed on a microscope slide and covered with a coverslip to keep it in place. Laser scanning confocal microscope was performed using the Nikon A1R RMP confocal microscope (Rouse Life Sciences Building,

Auburn University). Maximum excitation wavelengths for 2', 7'-dichloroflurescin and PI were 536 and 494, respectively. Green and red fluorescence signals were collected at the passbands of 505 to 525, and 610 to 650. In most cases, Z-series (overlay projections) were produced, i.e., several images were taken at different focal planes and overlays were produced with NIS-Elements program.

Bioinformatics

Cotton (*G. hirsutum*) breeding lines that are nominally susceptible, resistant, and hypersensitive to infection by RN have been established (McCarty 2017). The resistant germplasm was established by introgressing RN resistance from *G. barbadense* into elite *G. hirsutum* germplasm and is referred to as the Barbren-713 lines (Yik and Birchfield 1984). Introgression of nematode resistance from another species, *G. longicalyx*, resulted in the Lonren-1 breeding line which exhibits symptoms reportedly similar to hypersensitivity to reniform nematode (Sikkens 2011). Root tissues of the susceptible varieties DPL90 and SG747 (pooled as the SUS samples), resistant Barbren-713 (BAR samples), and hypersensitive Lonren-1 (LON samples), from both RN infected (SUS-I, BAR-I, and LON-I) and uninfected (SUS-U, BAR-U, and LON-U) plants were used for sequencing. Total RNA was prepared from root tissue, and submitted for transcriptome sequencing at the Hudson-Alpha Institute in Huntsville, AL. Using an Illumina HiSeq sequencer as reported previously (Li *et al.* 2015). The 100-bp Illumina transcriptome reads from all samples were assembled against the cotton genome sequence (Li *et. al.* 2015) using the Trinity RNA seq De Novo Assembly program v 2.4.0 (Grabherr 2015) to generate a Trinity genome guided transcriptome sequence assembly. This assembly consisted of 381308 individual transcripts "isoforms" that corresponded to 147867 unique genes that mapped

to the *G. hirsutum* genome. The assembly had a N50 = 1268, and 47326 of the transcripts mapped to known cotton gene sequences with at least 70% coverage of the corresponding known cotton genes.

1.16 RESULTS

The true nature of hypersensitive cell death (HCD) in plant roots (e.g., cotton Lonren-1) in response to PPN infection is still elusive. To determine, at the molecular and cellular levels, if the root-associated HCD is part of a plant defense machinery (PCD) or damage-related symptom (LCD), we have employed a confocal microscopy technique to observe the real time interactions and cellular responses of live plant roots during PPN infections.

Root cells of Lonren-1 do not activate HR in response to RN infections.

As an initial step to investigate if plant roots develop HR to fend off PPN infections, we retrieved and stained cotton roots with propidium iodide (PI) and 2',7'-dichlorodihydrofluorescein diacetate at 2-week post RN infections (Fig. 9, hypersensitive). Note that our early studies determined that a majority of RN will penetrate and establish in root tissues in approximately 13-16 days post inoculation (Jeffery 2017). It was immediately noticeable that secondary roots of infected Lonren-1 (hypersensitive), Barbren-713 (tolerant), and SG-747 (susceptible) accumulate H_2O_2. It was originally expected that H_2O_2 productions would only be prevalent around infection sites, but Barbren-713 and SG-747 displayed that H_2O_2 productions occur all over roots in a seemingly random pattern. Unexpectedly, Lonren-1 produced only a small amount of H_2O_2 during the infection of RN. Since H_2O_2 bursts are considered as a hallmark of HR development, the lack

of H_2O_2 accumulation in Lonren-1 speculated that the previously reported HCD might not be "true" PCD.

Indeed, there was no cell death throughout roots of all three germplasms at and near the infection sites. For instance, we were able to find pregnant female RN (e.g., please see the RN-infected root of Lonren-1) without causing apparent cell death at the neighboring cells. Considering that pregnancy takes a few days from the infection (J2) stage, the absence of developing cell death at the site of infection clearly concluded that the roots of Lonren-1 are incapable of developing PCD (HR) against RN infections.

Barbaren-713, a tolerant germplasm, produces a larger number of root hair vs. Lonren-1 and SG-714.

While monitoring H_2O_2 bursts and cell death in the roots of three cotton germplasms, it was apparent that the tolerant line Barbren-713 exhibited a thick mass of root hairs all along the secondary root. In contrast, hypersensitive line Lonren-1 displayed a less amount of root hairs, whereas susceptible line SG-747 had few, perhaps no root hair growth. However, in all infected cotton germplasms, root hairs had not disappeared completely, suggesting that RN infections cause root hair loss. When RN infections occur, a plant may redirect its resources from growth to defense mechanisms, stunting root hair development.

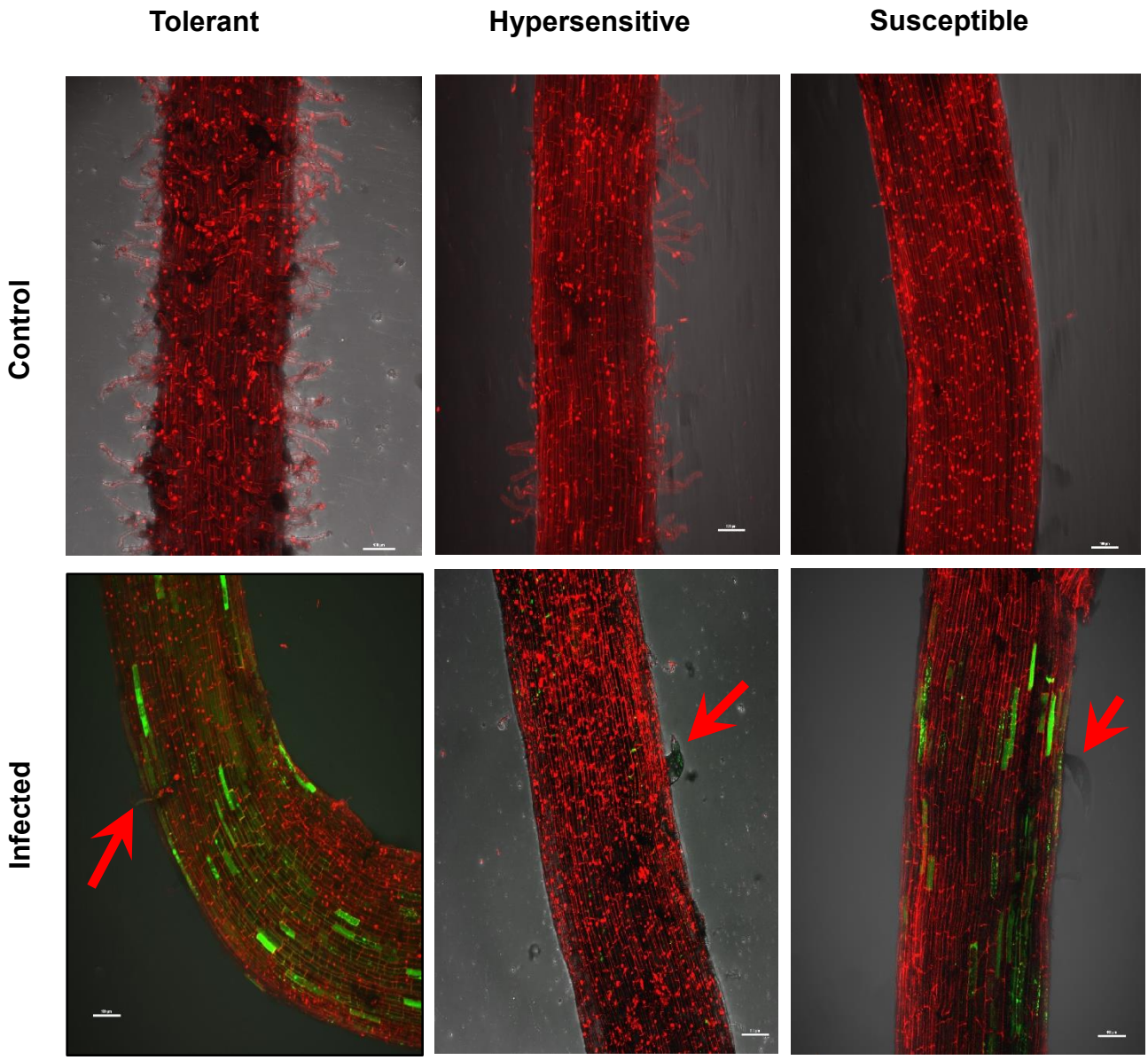

Figure 12: Reniform nematode infections cause H_2O_2 bursts but no HR (PCD). Roots of tolerant (Barbren), hypersensitive (Lonren-1), and susceptible (SG-747) cotton germplasms were visualized under a confocal microscopy after staining with PI (red, intact cell membrane) and H_2DCFDA (green, ROS). Arrows indicate root infected RN.

Bioinformatics analysis

Moving forward, we have employed a systematic biology approach to discern **i**) the tolerance associated genes and **ii**) if those genes are involved in root morphology by analyzing differential transcriptomes between the tolerant and susceptible germplasms before and after nematode infections. As an initial step level differences of transcripts between tolerant (Barbren-713, Bar0) and susceptible (SG-747, DSO), and hypersensitive (Lonren-1, L10) germplasms were established via the National Center for Biotechnology Information (NCBI) database and Blast2GO software. Since most of genes found in the results of DSO v. L10 are likely irrelevant (or negative) to tolerance phenotype, we are now subtracting those genes from the results of DSO v. Bar0. In addition, we have been generating a comprehensive list of genes related to root growth and root hair development based on a *Arabidopsis* database and identifying their homologues in cotton plants and analyzing their expression levels in Bar0 compared to DSO and L10.

Molecular function GO annotations between susceptible (DSO) germplasm and tolerant (Bar0) germplasm had the most differentially expressed transcripts of ATP binding, nucleotide binding and hydrolase binding. Biological process GO annotations between the two have differentially expressed transcripts of oxidation-reduction process, phosphorylation and transmembrane transport. Molecular function GO annotations between DSO germplasm and Lonren-1 hypersensitive (L10) germplasm have the most differentially expressed transcripts of ATP binding, metal ion binding and DNA binding. Biological process GO annotations in the same two are translation, transmembrane transport and defense response.

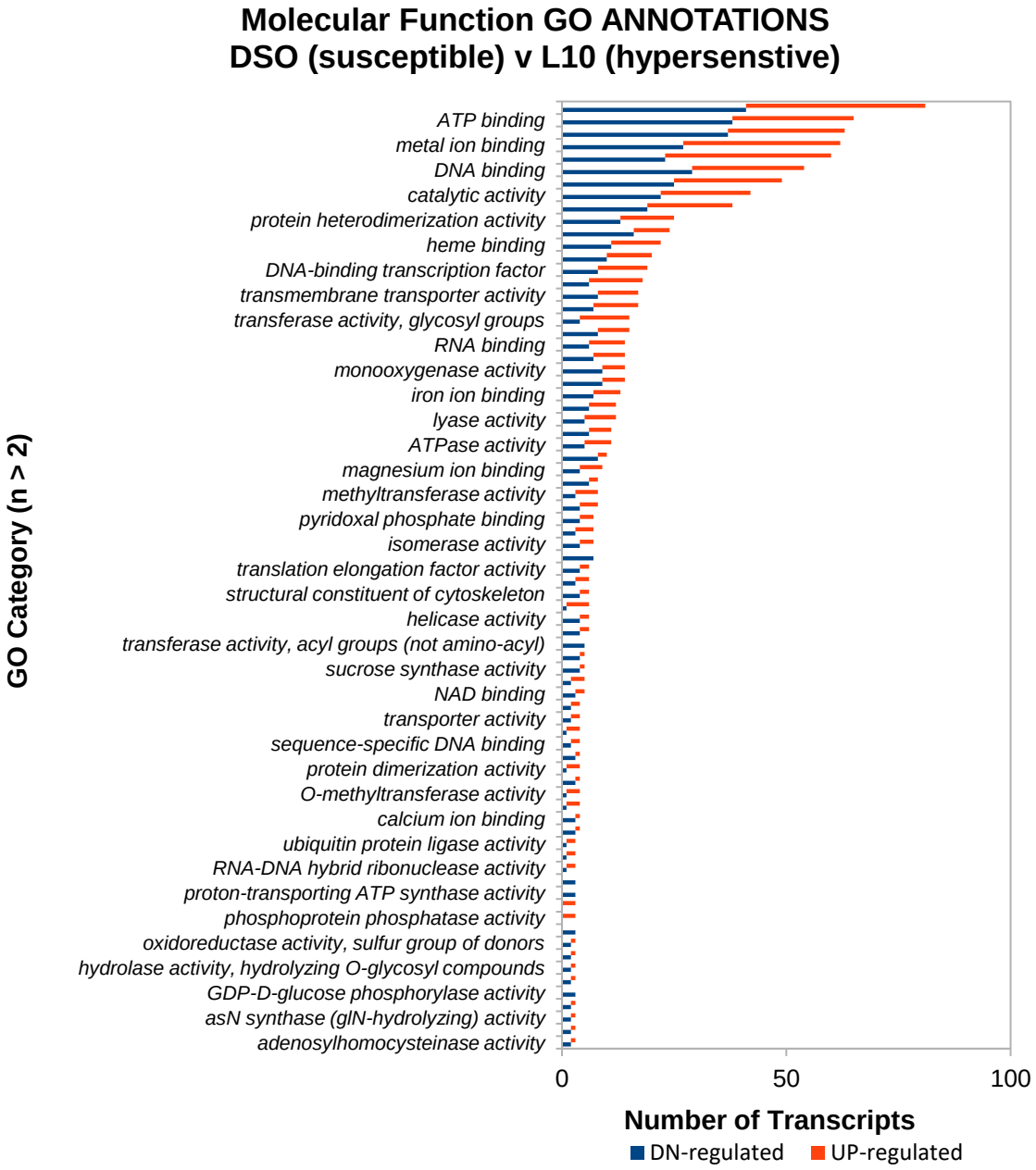

Figure 13: DSO v L10 Molecular Function. Molecular function GO annotations displays the most differentially expressed transcripts between SG-747 susceptible (DSO) line and Lonren-1 hypersensitive (L10) line is ATP binding, metal ion binding and DNA binding.

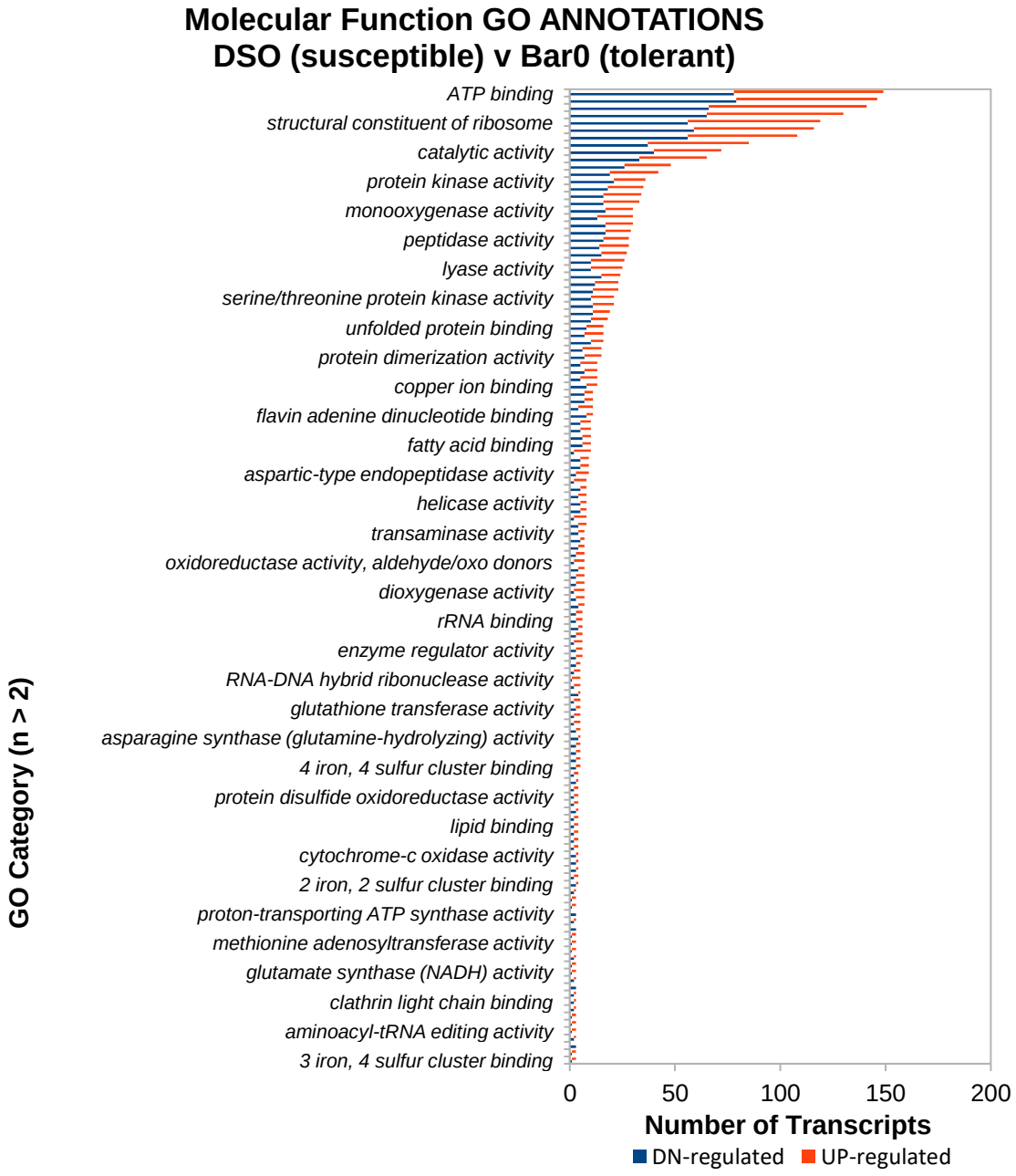

Figure 14: DSO v Bar0 Molecular Function. Molecular function GO annotations displays the most differentially expressed transcripts between SG-747 susceptible (DSO) line and Barbren-713 tolerant (Bar0) line is ATP binding, nucleotide binding and hydrolase binding.

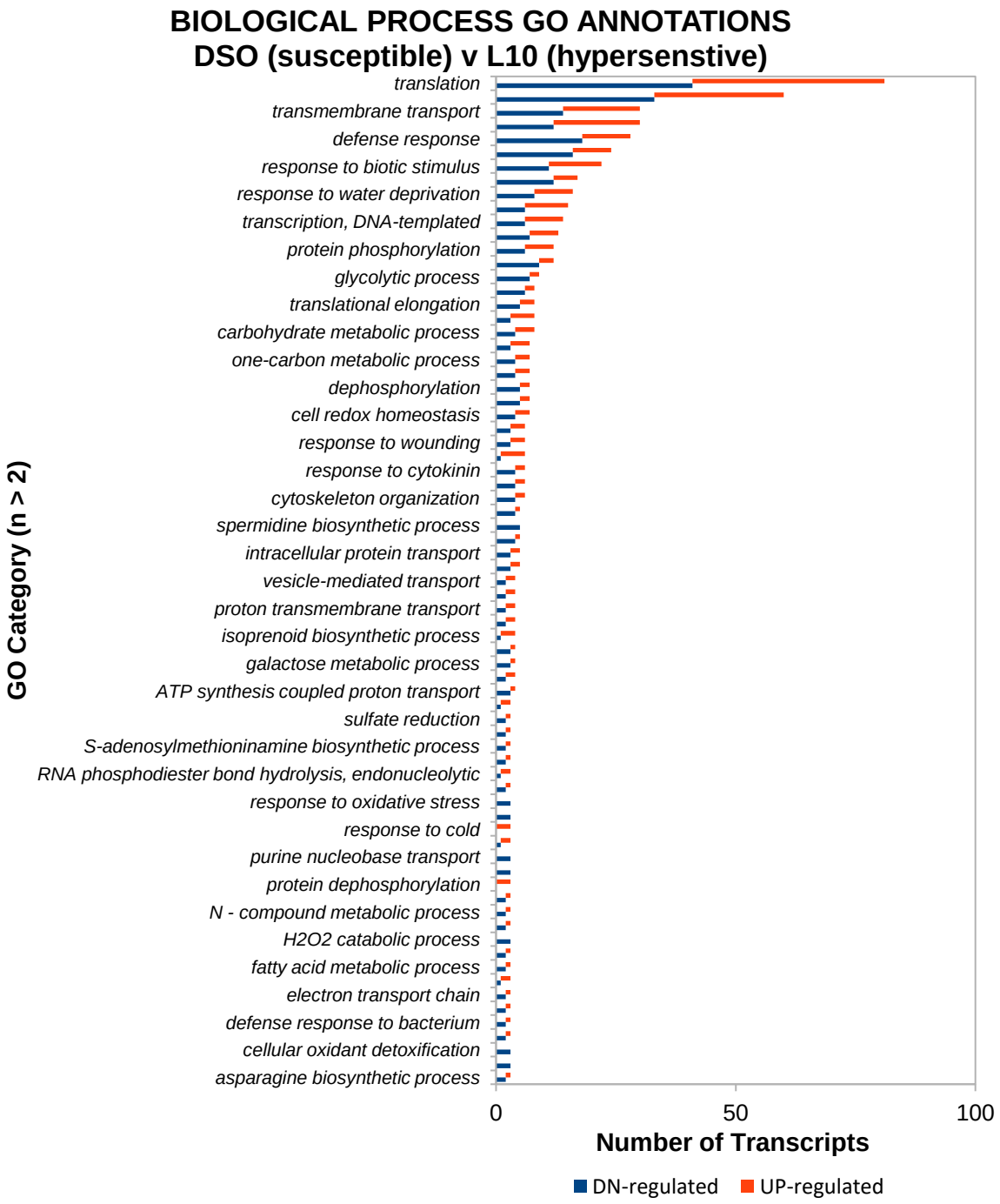

Figure 15: DSO v L10 Biological process. Biological process GO annotations displays the most differentially expressed transcripts between SG-747 susceptible (DSO) line and Lonren-1 hypersensitive (L10) line is translation, transmembrane transport and defense response.

Figure 16: DSO v Bar0 Biological process. Biological process GO annotations displays the most differentially expressed transcripts between SG-747 susceptible (DSO) line and Barbren-713 tolerant (Bar0) line is oxidation-reduction process, phosphorylation and transmembrane transport.

1.17 DISCUSSION

As an initial step to understand the modes of defense responses in plant (e.g., cotton) roots towards PPN infections, we have investigated PPN-associated HCD in plant roots, long hypothesized as PCD (HR). Recent studies have underpinned that PPN secrete conserved molecules, ascarosides, that are capable of eliciting PAMP (pathogen-associated molecular pattern) responses (referred to PAMP -triggered immunity, PTI) in various plants (Manosalva et al. 2015). In addition, these results perhaps shed new light on the role of phytonematode-derived cell-wall degrading enzymes (CWDE), which could activate the production of damage-associated molecular patterns (DAMP). This targeting to nucleotide binding domain leucine rich repeat protein (NB-LRRs) leading to ETI, induces several downstream signaling events such as Protein phosphorylation/dephosphorylation, ion fluxes and ROS production such as superoxide H_2O_2 during plant immune responses (Gillet 2017). Secondary signaling molecules or hormones such as salicylic acid and jasmonates are also produced, which in turn activate late defense genes (such as PR genes including *RP-1* and defensin genes). This then leads to defense mechanisms such as HR and callose deposition.

A single dominant gene (*Mi-1*) conferring resistance against the root-knot nematode *Meloidogyne* spp. was isolated over half a century ago from a tomato relative (*Lycopersicon peruvianum*, Bailey 1941). Since then, the major research goals of plant-nematode interactions have focused on espying PPN-derived avirulence (*avr*)-genes (also called effectors) that bind and trigger resistance (*R*)-gene (e. g. *Mi-1*)-mediated resistance (also called effector-triggered immunity, ETI). It has long been proposed that hypersensitive response transpires in cells located near invading PPN (Rice et al. 1985). Microscopic imaging observed a layer of necrotic cells at the periphery of syncytium produced upon phytonematode infection, and those cell deaths were

greater in resistant vs. susceptible potato lines although the reactions were comparatively slower than the typical HR. Since then, several studies have frequently monitored similar, if not the same, HR-like responses in various plant cells towards phytonematode infections (Anthony *et al*. 2005, Agudelo *et al*. 2005, Khallouk *et al*. 2011, Cabasan *et al.* 2014) in parallel with accumulations of reactive oxygen species (ROS) and phenolic compounds, classic chemical signals of HR (Waetzig et al. 1999, Pegard et al. 2004, Melillo et al. 2006, 2011, Simmonetti et al. 2009).

Roots of tolerant (Barbren), hypersensitive (Lonren-1), and susceptible (SG-747) cotton lines were visualized under a confocal microscopy after staining with propidium iodide (red, intact cell membrane) and 2',7'-dichlorofluorescein D (green, reactive oxygen species). After observing and capturing images of PPN-plant interactions, it was discovered there was a correlation of root development and tolerance when comparing Barbren root hairs before and after infection to Lonren-1 and SG-747 root hairs. To further investigate the importance of root hair growth/development as a precaution defense mechanism of cotton roots against PPN infections, a systematic biology approach was employed to determine if root organogenesis is differentially regulated between tolerant and susceptible germplasms before and after nematode infection. Note that current and initial analyses were yet incomplete to reveal those genes. However, current results revealed that the transcripts of ATP binding, nucleotide binding, hydrolase binding, oxidation-reduction process, phosphorylation and transmembrane transport are significantly upregulated in the roots of Barbren-713 tolerance germplasm. Besides, transcripts of ATP binding, metal ion binding and DNA binding were highly upregulated in SG-747 susceptible germplasm vs. Lonren-1 hypersensitive germplasm. Together, these studies reject that PPN in tolerant, susceptible and hypersensitive cotton germplasms cause HR and suggest that ROS productions are not prerequisite of HR. As of now, our study suggests the importance of root hair growth and/or root development,

perhaps re-recognizing plant-PPN interactions as plant-insect/herbivore interactions rather than plant-microbe interactions.

To further substantiate our results, we will employ DeadEnd^{TM} Colorimetric TUNEL system in the future. The TUNEL assay (from Promega Corporation, 2800 Woods Hallow Road, Madison WI) is a non-radioactive system designed to provide simple, accurate and rapid detection of apoptotic cells in situ at the single-cell level. The system is used to assay apoptotic cell death in tissue sections, measuring nuclear DNA fragmentation, an important biochemical indicator of apoptosis in many cell types. This assays together with our present results then clarify that HR does not occur in plant roots against PPN infections.

1.18 LITERATURE CITED

Agudelo P., R. T. Robbins, J. M. Stewart, A. Bell, and A.F. Robinson. 2005. Histological observations of Rotylenchulus reniformis on Gossypium longicalyx and interspecific hybrids. J. Nematol 37:444–447.

Anthony F, P. Topart, A. Martinez, M. Silva, M. Nicole. 2005. Hypersensitive-like reaction conferred by the Mex-1 resistance gene against *Meloidogyne exigua* in coffee. Plant Pathol 54: 476-482.

Bailey D. M. 1941. "The seedling method for root-knot nematode resistance". *Proceedings of the American Society for Horticultural Science.* 38: 573-575.

Cabasan M. T. N., A. Kumar, S. Bellaflore, D. De Waele. 2014. Histopathology of the rice root-knot nematode, *Meloidogyne graminicola*, on *Oryza sativa* and *O. glaberrima*. Nematology 16: 73-81.

Castagnone-Sereno P, J. P. Semblat, C. Castagnone. 2009. Modular architecture and evolution of the *map-1* gene family in the root-knot nematode *Meloidogyne incognita*. Mol Genet Genomics 282: 547-554.

Doshi R. A., R. L. King, G. W. Lawrence. 2010. Classification of *Rotylenchulus reniformis* numbers in cotton using remotely sensed hyperspectral data on self-organizing maps. J Nematol 42: 179-193.

Fosu-Nyarko J, M. J. K. Jones. 2016. Advances in understanding the molecular mechanisms of root lesion nematode host interactions. Annu Rev Phytopathol 54: 253-278.

Gillet F. X., *et al*. "Plant-parasitic nematodes: towards understanding molecular players in stress responses". *Annals of Botany* 119.5 (2017): 775-789.

Gleason C.A., Q. L. Liu, V. M. Williamson. 2008. Silencing a candidate nematode effector gene corresponding to the tomato resistance gene *Mi-1* leads to acquisition of virulence. Mol Plant Microbe Interact 21: 576-585.

Hwang C.F., A. V. Bhakta, G. M. Truesdell, W. M. Pudlo, V. M. Williamson. 2000. Evidence for a role of the N terminus and leucine-rich repeat region of the Mi gene product in regulation of localized cell death. Plant Cell 12: 1319-1329.

Jeffrey, R. A. 2017. Cellular elucidation of mode of defense responses in cotton roots in response to *Rotylenchulus reniformis* infections. Department of Entomology and Plant Pathology, Auburn University, AL.

Khallouk S, R. Voisin, C. Van Ghelder, G. Engler, S. Amiri, D. Esmenjaud. 2011. Histological mechanisms of the resistance conferred by the Ma Gene Against *Meloidogyne incoggnita* in *Prunus* spp. Phytopathology 101: 945-951.

Lozano-Torres J. L., R. H. P. Wibers, P. Gawronski, J. C. Boshoven, A. Finkers-Tomczak, J. H. Cordewener, A. H. America, H. A. Overmars, J. W. Van ‘t Klooster, L. Baranowski, M. Sobczak, M. Ilyas, R. van der Hoorn, A. Schots, P. J. de Wit, J. Bakker, A Goverse, G. Smant. 2012. Dual disease resistance mediated by the immune receptor CF-2 in tomato requires a common virulence target of a fungus and a nematode. Proc Natl Acad Sci USA 109: 10119-10124.

Melillo M.T., P. Leonetti, M. Bongiovanni, P. Castagnone-Sereno, T. Bleve-Zacheo. 2006. Modulation of reactive oxygen species activities and H_2O_2 accumulation during compatible and incompatible tomato-root-knot nematode interactions. New phytol 170: 501-512.

Melillo M.T., P. Leonetti, A. Leone, P. Veronico, T. Bleve-Zacheo. 2011. ROS and NO production in compatible and incompatible tomato-*Meloidogyne incognita* interactions. Eur J Plant Pathol 130: 489-502.

Mitchum M. G., et al. 2013. "Nematode effector proteins: an emerging paradigm of parasitism". *New Phytologist Journal.* 199.4: 879-894.

Mur L.A., P. Kenton, A. J. Lioyd, H. Ougham, E. Prats. 2008. The hypersensitive response; the centenary is upon us but how much do we know? J Exp Bot 59: 501-520.

National Cotton Council of America (NCCA). 2015. NCC Comments on Pollinator Proposal.

Pegard A, G. Brizzard, A. Ffazari, O. Soucaze, P. Abad, C. Djian-Caporalino. 2001. Histological characterization of resistance to different root-knot nematode species related to phenolics accumulation in *Capsicum annuum*. Phytopathology 95: 158-165.

Promega Corporation. 2018. DeadEnd™ Colorimetric TUNEL system: Instructions for use of products G7130 and G7360. 2800 Woods Hollow Road. Madison, WI, USA.

Rice S.L., B. S. C. Leadbeater, A. R. Stone.1985. Changes in cell structure in roots of resistant potatoes parasitized by potato cyst-nematodes. I. Potatoes with resistance gene H_1 derived from *Solanum tuberosum* ssp. *andigena*. Physiol Plant Pathol 27: 219-234.

Sacco M. A., K. Koropacka, E. Grenier, M. J. Jaubert, A. Blanchard, A. Goverse, G. Smant, P. Moffett. 2009. The cyst nematode SPRYEC protein RBP-1 elicits Gpa2-and RanGAP2-dependent plant cell death. PLoS Pathogens 5: e1000564.

Santana B.P., F. Nedel, C. Perelló Ferrú, R. Marques e Silva, A. F. da Silva, F. F. Demarco, N. Lenin Villarreal Carreño. 2015. Comparing different mothods to fix and to dehydrate cells on alginate hydrogel scaffolds using scanning electron microscopy. Microsc Res Tech 78: 553-561.

Sikkens, R.B., D. B. Weaver, K. S. Lawrence, S. R. Moore, E. van Santen. 2011. Lonren plant cotton germplasm response to *Rotylenchulus reniformis* inoculum level. Nematropica 41:68.

Steiner, G. 1925. The problem of host selection and host specialization of certain plant-infesting nemas and its application in the study of nemic pests. Phytopathology 15:499-534, illus.

Vos, P., G Simmones, T. Jesse, *et al*. 1998. The tomato Mi-1 gene confers resistance to both root-knot and potato aphids. Nat Biotechnol 16 (13): 1365-9.

Waetzig G. H., M. Sobczak, F. M. W. Grundler. 1999. Localization of hydrogen peroxide during the defence response of *Arabidopsis thaliana* against the plant-parasitic nematode *Heterodera glycines*. Nematology 1: 681-686.

Weaver D. B. 2015. Cotton nematodes. Pp. 547-570 *in* DD Fang, RG Percy ed. Cotton. 2nd. ASA, CSSA, and SSSA, Madison, WI, USA.

Williamson V.M., A. Kumar. 2006. Nematode resistance in plants: the battle underground. Trends Genet 22: 396-403.